# Floods and Droughts in the Murray-Darling Basin: New Insights from Lake Alexandrina

Calum McRae

November 2019


THE UNIVERSITY of ADELAIDE

# Floods and Droughts in the Murray-Darling Basin: New Insights from Lake Alexandrina.

## LAKE ALEXANDRINA SEDIMENTS

## ABSTRACT

A study on the sediments of Lake Alexandrina, a lake located at the terminus of the River Murray in the Lower Lakes Region, South Australia, is presented in attempts to reconstruct the flow regime of the River Murray throughout the last 4000yr BP. $\delta^{18}O$ and Itrax data are used as environmental proxies and $^{210}Pb$ and $^{14}C$ techniques are used to construct age-depth models and infer accumulation rate.

Recent, $^{210}Pb$-based accumulation rates of 1.5-1.57cm/yr are greater than those gathered from $^{14}C$ which gave an accumulation rate of 0.1cm/yr. This change is attributed to European settlement.

$\delta^{18}O$ reveals a fresh-water dominated history with a mean value of -8.24488. Itrax ratios of Al and Si show links to grainsize. Thus Itrax data is used for high resolution paleo flow reconstructions. $\delta^{18}O$ and Itrax data agrees in some stretches, but not all. A dry event between 4.0ka and 3.5ka captured by Al/Si also appears in several similar paleo limnologic reconstruction for lakes throughout south east Australia. Wavelet analysis of Al/Si does not display climatic oscillation thought to be typical of the region, such as the el Niño Southern Oscillation and the Indian Ocean Dipole. The Gleissberg cycle appears to effect the lakes hydrology between ~4.0Ka and ~2.6Ka.

## KEYWORDS

Floods, Droughts, Lak Alexandrina, 14-C, 210-Pb, Chronology, 18-Oxygen

**TABLE OF CONTENTS**

## LIST OF FIGURES AND TABLES

## INTRODUCTION

Floods and droughts are two of the most economically devastating natural phenomena worldwide. Floods alone have been estimated to cost the global community approximately US$1 trillion per year (Hallegatte, Green, Nicholls, & Corfee-Morlot, 2013), with the frequency and severity of such climatic events believed to increase in coming years due to climate change (*Climate Change 2007 - Impacts, Adaption and Vulnerability*, 2007). For such reasons, it is empirical to attempt accurate and reliable models indicating the frequencies of such events. There has been recent emphasis on the inclusion of paleo-data for flood magnitude and frequency analysis as well as broader climate models. N. Macdonald, Kjeldsen, Prosdocimi, and Sangster (2014) show that the inclusion of historical data could reduce uncertainty by up to 40% in their models whilst Ault et al. (2014) suggest contemporary climate models such as CMIP5 significantly underestimate the amplitude of extreme drought events, largely due to the narrow temporal scope of the data they were built upon.

For such reasons, this study aims to create a continuous, qualitative record of Murray River flow via a core representing 4000 years of sedimentation in Lake Alexandrina. The sediments of Lake Alexandrina are sensitive to changes throughout the Murray-Darling basin with an estimated 50% of flow from the River Murray and Darling River reaching the Murray Mouth under natural conditions (Gell, Tibby, Baldwin, & Hancock, 2007; K. Walker, 2006). Thus, basin-wide paleo-hydrology can be inferred. Existing palaeolimnological analysis indicates predominantly fresh-water conditions in Lake Alexandrina from *ca* 6000 yr BP. This conjecture is largely derived from diatom assemblages (Barnett, 1994; Fluin, Haynes, & Tibby, 2009). This is seen to indicate the development and stabilisation of the Younghusband Peninsula (or some preliminary

form thereof) which separates the lower lakes from the Southern Ocean. Diatom flora also indicate increasing freshwater flows since this period (Fluin, Haynes, & Tibby, 2009). $\delta^{18}O$ values obtained in this study can be used to verify the freshwater nature of Lake Alexandrina during this time. The greatest and most ubiquitous change to diatom assemblages in Lake Alexandrina occur following European colonisation (Barnett, 1994; Fluin, Gell, Haynes, Tibby, & Hancock, 2007). $^{201}Pb$ and $^{14}C$ chronologies have also been used to infer increased sedimentation rate following European settlement within Lake Alexandrina and various wetlands throughout the MDB (Barnett, 1994; Gell et al., 2009).

What existing studies lack however, are high quality chronologies and high resolution data. Barnett (1994) only uses 4 radiocarbon dates to construct a 7000 year age depth model. Additionally, Gell et al. (2009) only use basal ages when examining Lake Alexandrina. By contrast, the $^{14}C$ chronology presented in this study uses a multitude of ages sampled near-evenly throughout depth. High resolution Itrax data is also used to create robust time series data. Such data can be used for wavelet analysis, unprecedented for Lake Alexandrina. The validity of Itrax data as an environmental proxy is gathered via the relationship between elemental ratios and grainsize. Grainsize is widely used to infer periods of high or low flow (*Li, Guo, & Yu, 2013; Thorndycraft, Hu, Oldfield, Crooks, & Appleby, 1998*), thus a meaningful relationship allows Itrax data to be used as a proxy for paleo-flow. $\delta^{18}O$ levels derived from cellulose will also be used to infer paleo-hydrology. Low $\delta^{18}O$ levels are seen to reflect periods of high rainfall as meteorologic $H_2O$ is depleted in $^{18}O$. Conversely, high $\delta^{18}O$ can reflect periods of low rainfall, either through seawater incursion as a result of low flow

(seawater being enriched in $^{18}O$ compared to meteorological water) or through evaporation which leaves the residual water enriched in $^{18}O$.

$^{210}Pb$ and $^{14}C$ chronologies are used to examine the effects of European colonisation on sedimentation rate. Plutonium levels will be examined, as a spike can be used as a chronological anchor reflecting the 1956, Mosaic-G2 nuclear weapons test in the South Pacific (B. S. Smith et al., 2016). Additionally, the appearance of *Pinus* pollen will be used to infer time of European settlement.

Under natural conditions, the flow regime of the River Murray varies as a function of the El Niño Southern Oscillation (ENSO) (Simpson, Cane, Herczeg, Zebiak, & Simpson, 1993). This relationship, however, is based exclusively on instrumental data. Ho, Verdon-Kidd, and Kiem (2014) used paleo proxies to examine climatic drivers for rainfall in various sub catchments of the MDB and found climatic oscillations such as the Indian Ocean dipole (IOD), Interdecadal Pacific Oscillation (IPO) and the Southern Annular Mode (SAM) as well as ENSO can explain the observed data for different sub catchments. For this reason, this study uses wavelet analysis to uncover links between flow regimes and climatic oscillations.

The climatic record of Lake Alexandrina is compared to similar models of lakes throughout south east Australia. This allows examination of regional climatic shifts. Inferred conditions between 4.0 Ka and 2.0 Ka differ depending on which sites are examined (Gingele et al., 2007; Gouramanis, De Deckker, Switzer, & Wilkins, 2013; Gouramanis et al., 2010; Kemp et al., 2012; Marx, Kamber, McGowan, & Denholm, 2011). Arid conditions, associated with reduced frequency of moisture rich south-westerly winds have been inferred after 2.0 Ka (Gouramanis et al., 2013; Marx et al., 2011).

## SITE DESCRIPTION


**Figure 1. Map of Lake the Lower Lakes region, South Australia, consisting of Lake Alexandrina, Lake Albert and the Coorong.**

Lake Alexandrina is a predominantly freshwater lake located approximately 50km south east of Adelaide. It covers approximately 600 square kilometres with a mean depth of 2m (Bourman & Barnett, 1996). Underlying the region are Neoproterozoic to Cambrian metasediments, Devonian to late carboniferous basinal sediments and Permian glacial deposits (Stephenson & Brown, 1989). The most basal Quaternary formation is the Coomandook Formation, comprising of calcareous sands and shallow marine, fossiliferous limestone. Overlying this lies the Bridgewater Formation which includes

Aeolian bioclastic sands and calcarenites (Bournman, Murray-Wallace, Belperio, & Harvey, 2000). The uppermost formation in the lower lakes sequence is the Holocene, St. Kilda formation, in which siliceous muds and sands are still being deposited. The majority of Lake Alexandrina's sediments are believed to be from the St. Kilda formation (Barnett, 1994).

Radiocarbon ages from basal sediments of the Lower lakes indicate the Lake formed between 7000 and 8000 yr BP (Fluin et al., 2007). Before this time, the area would have been significantly inland as a result of sea level lowstand. As sea-levels rose during that last marine incursion, the mouth was pushed inland until stabilising at its current location ca. 7000 yr BP (Barnett, 1994).

Natural River Murray discharge varies seasonally with a high during late winter to spring and a low during late summer (K. F. Walker, 1985). Through a series of barrages, dams and weirs, water levels have been kept relatively stable throughout the 20$^{th}$ Century. River regulation has increasingly masked the aforementioned fluctuations (K. Walker, 2006).

## METHODS

A 5m core (LA009) was taken using a rod operated piston corer in 2009. The core was extracted close to the River Murray inlet in an area protected by a sand spit, mitigating problems associated with scouring and turbation. The core was divided into five 100cm sections. The shallowest section, representing 0-100cm was lost during transport between universities. A second expedition in 2017 was conducted to replace this section (LA009/17). A 30cm gravity core (LAG) was also taken at this time. Efforts were made

to ensure the site for the second expedition was as close as possible to the first. LA009 and LA009/17 shrunk due to water loss since collection. The following equation was used to correct for shrinking:

$$D_{original} = D_{Current} \frac{L_{original}}{L_{current}} \quad (1)$$

Where $D$ = depth of sample and $L$ = total length of core.

A preliminary 14C age-depth model of the core existed prior to this study, however 2 dates were added to resolve ambiguity. Samples used in the existing age model were obtained from wood, if present. If no wood was present at the desired depth, seeds were used, if no seeds were present, grassy material was used. Wood samples were collected in this study. Preparation and analysis were conducted at ANSTO, Lucas Heights following standard procedure outlined in appendix A. Acid-alkali-acid pre-treatment was done as outlined by Hau, Barbetti, Jacobsen, Zoppu, and Lawson (2000). The sealed-tube combustion technique was used for CO2 extraction, outlined by (Vandeputte, Moens, & Dams, 1996) and graphitization was done by reducing graphite over an iron catalyst at high temperatures (600°C) in the presence of excess $H_2$ (Vogel, Southon, Nelson, & Brown, 1984). $^{14}C$ ages were obtained using the Lucas Heights accelerated mass spectrometer, the details of which can be found in Tuniz et al. (1994). The carbon ages were fed into the r package 'Bacon', using the Southern Hemisphere carbon calibration curve, to construct an age depth model (Blaauw & Christen, 2011). Bacon was chosen over linear or spline interpolation as these approaches treat $^{14}C$ ages as single points. In reality, imposing the Gaussian $^{14}C$ distribution gathered via AMS over a carbon calibration curve returns asymmetric, often multi-peaked probability densities. Bacon treats the $^{14}C$ ages as such and generates a multitude of interpolations using points randomly generated from said densities.

Samples for $^{210}$Pb and Plutonium were taken from LAG, as the gravity cores preserve surface sediments more reliably than piston cores (Skinner & McCave, 2003). The principles of $^{210}$Pb dating can be found in Appleby and Oldfield (1978). Isolation of $^{226}$Ra and $^{210}$Po from samples were conducted following processes outlined in appendices B and C. The Ortec Alpha-Esemble-8, fitted with Silicon Charged Particle Radiation Detectors was used to obtain $^{210}$Po levels. Alpha emitting radionuclides with certified activities consistent with the National Institute of Standards and Technology (NIST) were used to determine efficiency and energy calibrations. $^{226}$Ra levels were obtained using the Ortec High Purity Germanium Gamma Ray detector. Gamma emitting radionuclides with certified values consistent with NIST were used for Efficiency and energy calibrations. $^{226}$Ra represents supported $^{210}$Pb and $^{210}$Po represents total $^{210}$Pb. Unsupported $^{210}$Pb, from which ages are determined, are gathered from subtracting supported $^{210}$Pb from total $^{210}$Pb. Dry bulk densities were obtained as outlined in appendix D. Ages were calculated from unsupported $^{210}$Pb via the constant initial concentration (CIC) and constant rate of supply (CRS) models as per Appleby and Oldfield (1978). Preliminary $^{210}$Pb ages informed selection of depths likely to display the Plutonium spike. Plutonium isolation was conducted following processes outline in appendix D. Plutonium samples were loaded into the VEGA 1MV accelerator system at ANSTO as per (Hotchkis et al., 2019).

Preliminary cellulose extraction attempts indicated large amounts of sediments were needed to produce a viable yield. Thus, every other 2cm section of LA009 and LA009/17 was sampled. Details of core sampling can be found in Appendix E. Cellulose extraction was conducted by immersing samples in Sodium chlorite overnight to remove organics. Samples were then left stirring in cuprammonium solution for 16

hours to dissolve cellulose. After the cellulose-cuprammonium solution was decanted, sulphuric acid was added to re-precipitate cellulose. The details of this method can be found in Wissel, Mayr, and Lucke (2008). The samples were loaded into a mass spectrometer for $\delta^{18}O$ analysis. Lakewater $\delta^{18}O$ is inferred under the assumption of aquatic-derived cellulose, using the following equation, described by Edwards and McAndrews (1989):

$$\delta^{18}O_{Water} = \frac{\delta^{18}O_{Cellulose}}{0.973} - 27.2‰ \quad (2)$$

Eq. (2) has been used extensively to infer the paleo hydrology of lakes with a variety of sediment types (Birks, Edwards, & Remenda, 2007; Edwards & McAndrews, 1989; G. M. MacDonald, Edwards, Moser, Pienitz, & Smol, 1993; Wolfe et al., 2000; Wolfe et al., 2005) and is appropriate as $\delta^{18}O$ fractionation between water and cellulose has been shown to be independent of temperature and species (DeNiro & Epstein, 1981; Epstein, P., & Yapp, 1977; Yakir & DeNiro, 1990). Standards ran with samples did not line up with their listed lab ID spot, meaning the labels for each data point were likely incorrect. To circumvent this issue, sample were listed by weight and then assigned values with correlating peak area, as larger samples should have proportionally large peak areas.

LA009 and LA009/17 were scanned using Itrax X-ray florescence giving high resolution values indicating changes in chemical abundance. As the distance between the detector and core drifts throughout analysis, Itrax values are only meaningful as ratios to one another. The ratios Al/Si, K/Si, Ca/Si, Al/Ti, Mg/Fe, Zr/Si, Ni/Si, Ni/Ti, S/Ti and S/Si were chosen due to their potential mineralogical significance. Slight collapse of sediment at the top and/or bottom of each core occurred when laid down for scanning. This inaccurate data was removed prior to this study, resulting in artificially

shortened lengths for each core. A decision was made to use Eq. (1) to 'correct' these lengths to 1m. Whilst inaccurate, it was impossible to determine how much length had been lost, leaving no alternative solution. Work on cellulose extraction had begun prior to grainsize analysis. During which, cores were bagged into 2cm intervals, making this the highest possible resolution for grainsize analysis. The Itrax values were therefore put into 2cm mean-averaged bins. To ensure the full range of Itrax values were present for grainsize analysis, script was created in r identifying bins containing the top and bottom 5% Itrax values. Middle values were obtained using the equation:

$$mid = \frac{max-min}{2} + min \quad (3)$$

A similar r script was created to identify bins within a bracket around this middle value. The bracket had to be tailored for each elemental ratio as a fixed ± value or percent yielded a different number of bins for each elemental ratio. This approach was chosen as median values did not lie near the centre of most Itrax ranges. Depths correlating to these bins were selected for grainsize analysis. Samples were immersed in the disaggregate, 5% sodium-hexametaphosphate overnight prior to analysis. Grainsize distribution was obtained using a Malvern Mastersizer 2000.

Wavelet transforms were chosen over methods such as Fourier transforms as wavelets can identify periodicity which only existed for finite stretches of time. As different climatic cycles are believed to vary as primary climatic drivers throughout time, detecting periodicity within various time windows is paramount. Prior to such analysis the data must be in a form where each data point is sampled uniformly in time. Script was created in r, which interpolated age verses elemental data and gave 4000 equally spaced data points. This data was then fed into PAST (Hammer, David, Harper, & Ryan, 2001) which ran a morlet wavelet transform. Morlet wavelets were used as the

time series shows little resemblance to a specific wave type, thus more tailored wavelet construction is unnecessary.

## OBSERVATIONS AND RESULTS

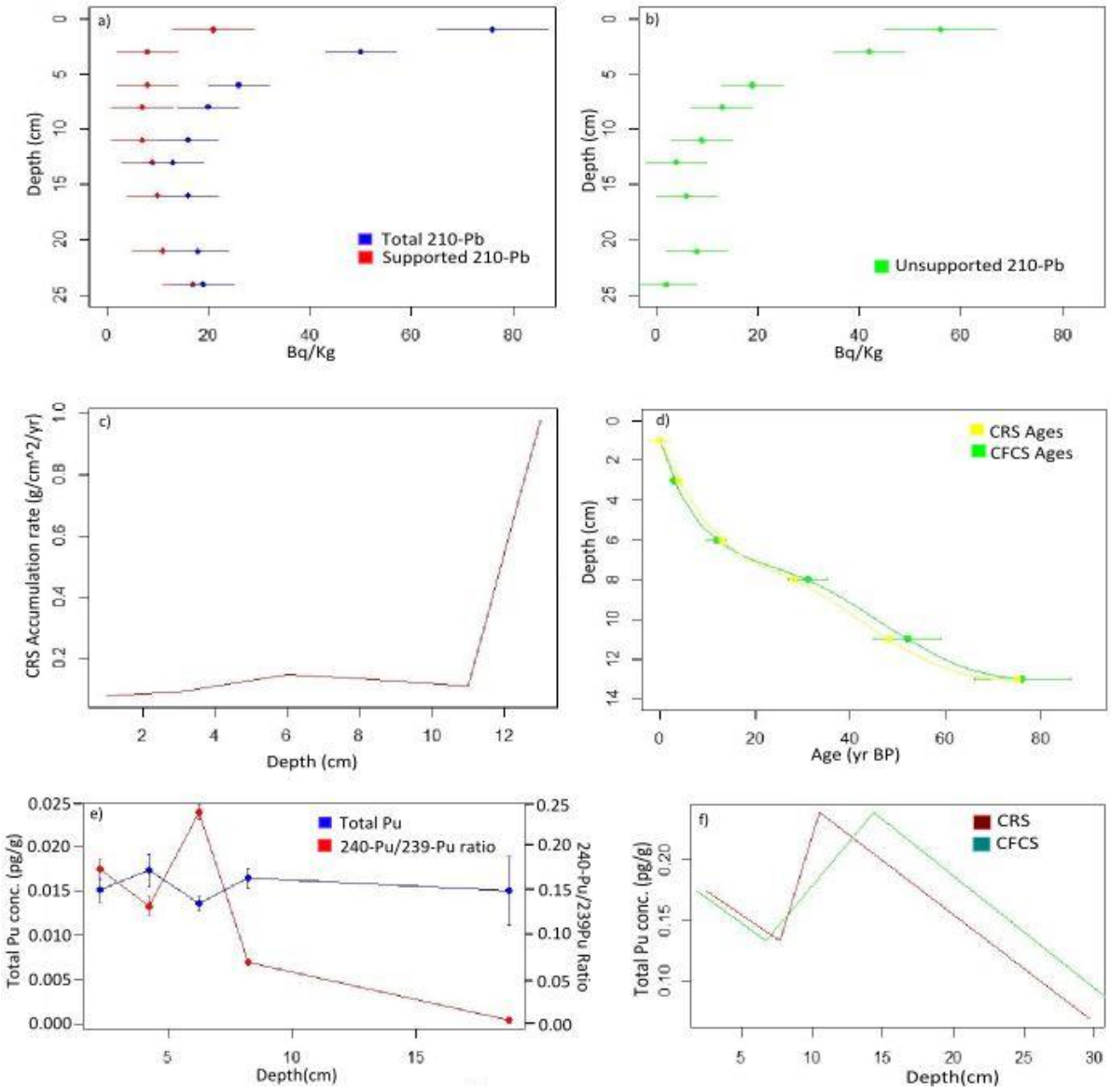


**Figure 2. 210-Pb and Pu results. a) Total 210-Pb (blue), derived from 210-Po. Supported 210-Pu (red), derived from 226-Ra. b) Unsupported 210-Pb calculated using: total – supported = unsupported. c) CRS accumulation rate as per Appleby and Oldfield (1978). d) CR**

Supported $^{210}$Pb ranges between 21Bq/kg and 7Bq/Kg. The shallowest value is the highest. Total $^{210}$Pb ranges between 76Bq/Kg and 13Bq/Kg. Total activty decreases

from 0cm to 13cm, after which, values drift. Unsupported $^{210}$Pb ranges between 56Bq/Kg and 2Bq/Kg. Unsupported $^{210}$Pb activities exhibit a decreasing profile with depth between 0 and 13cm. 13cm correlates with a CFCS age of 76yr BP and a CRS age of 75yr BP. Beyond this date, ages cannot be interpoloated. $^{240}$Pu/$^{238}$Pu ranges between 0.0239pg/g at 6.25cm depth and 0.0004pg/g at 18.25cm depth. Total Pu concentration could only be graphed between 0 to 32.75yr Bp for CFCS and 0 to 29.67yr Bp as the sample at depth 18.75 cm lies outside the interpolation brcaket. *Pinus* pollen first appears at 27cm depth. The appearance of *Pinus* pollen and the 1956 Mosaic weapons test both lay outside the interpolated age bracket.

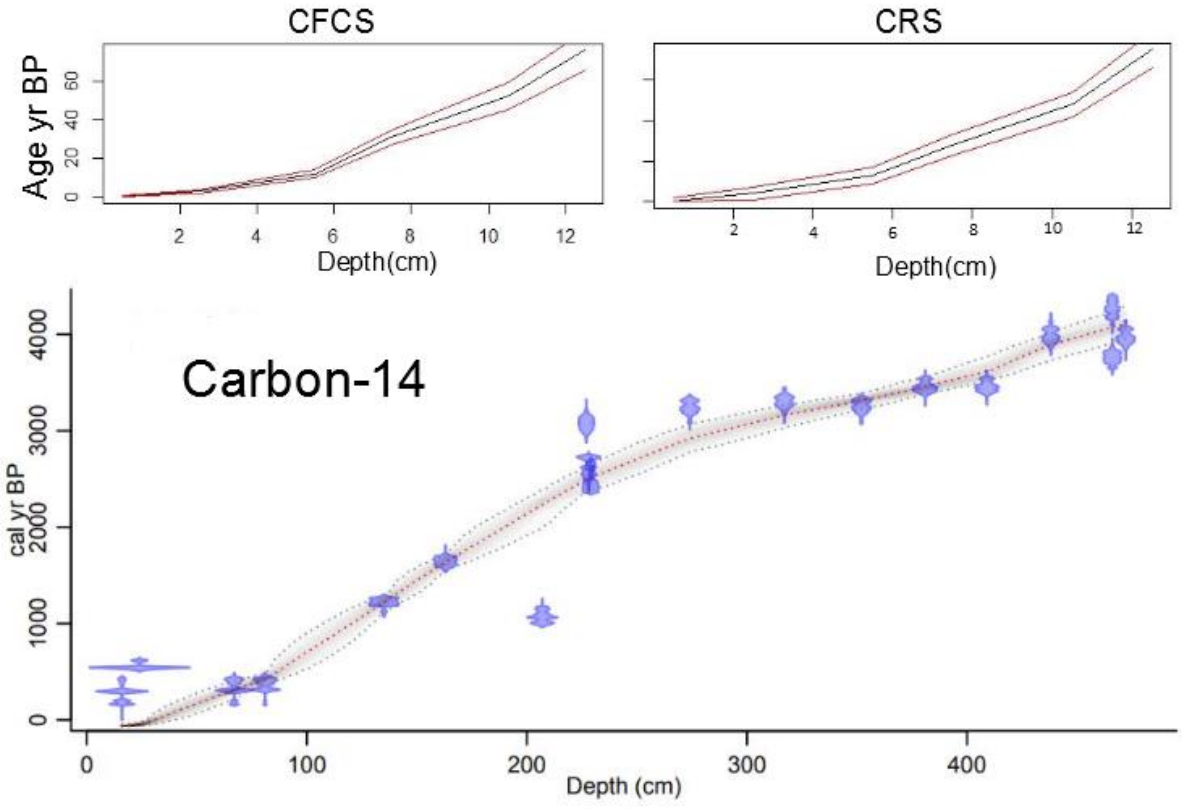


**Figure 3. Constant flux, constant sedimentation (CFCS) model and Constant rate of supply (CRS) 210-Pb age depth models shown above. Carbon-14 samples derived from various plant matter. Carbon-14 age depth model created using rBacon**

CFCS and CRS derived $^{210}$Pb dates show similar trends. CRS ages have a larger margin of error, especially for shallower depths. CFCS decreases its rate of change between 6cm and 8cm whereas CRS has a constantly increasing rate of change between points. $^{14}$C ages shallower than 250cm show a lower sedimentation rate than ages deeper than

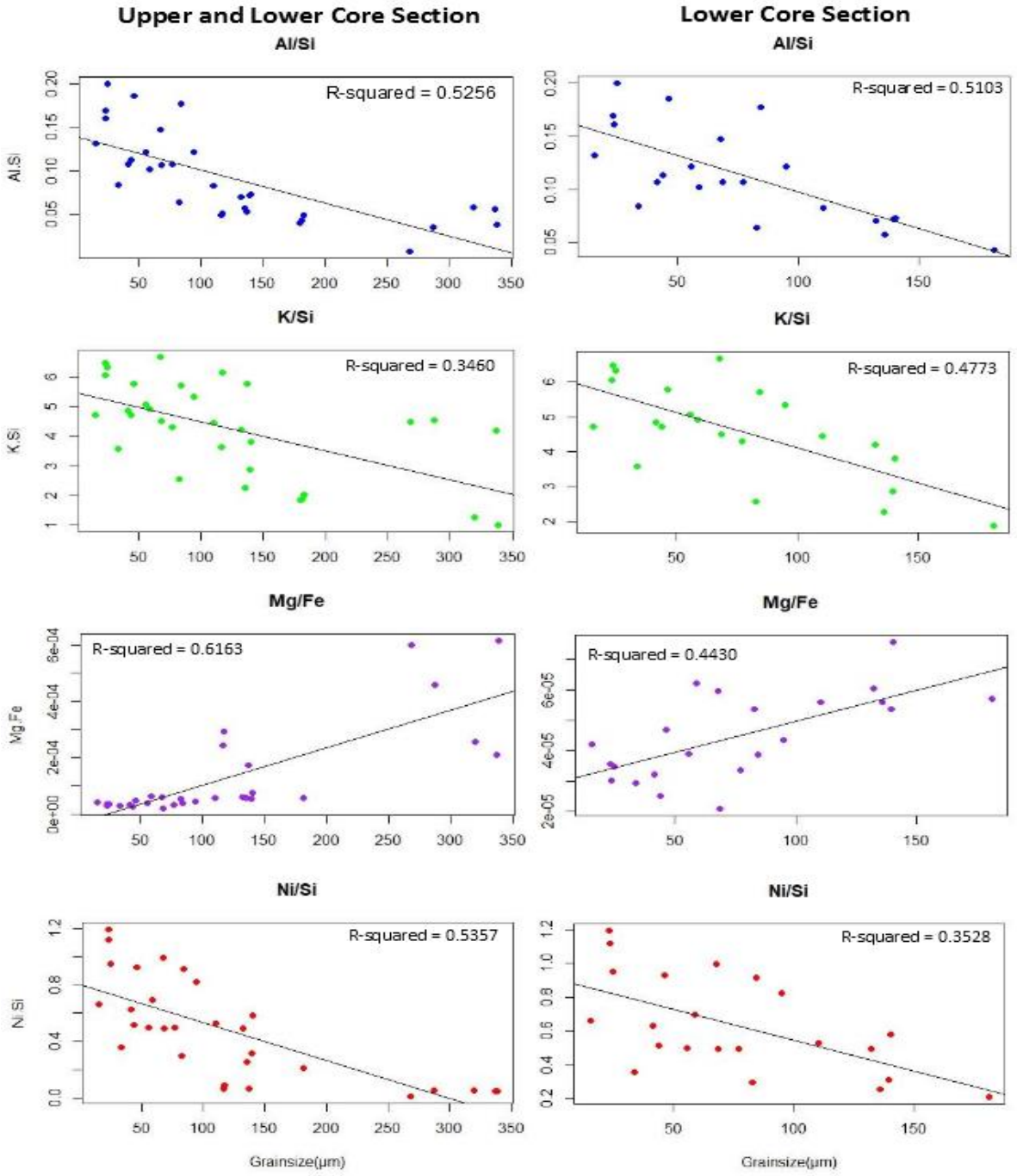


**Figure 4. Elemental Itrax ratios versus depth. Graphs in the left column use all points gathered for grainsize. Graphs in the right column exclude data from LA009/17.**

250cm. Several clear outliers exist, including the shallowest two points and the point at ~210cm depth. All other ages sit relatively comfortably along the age-depth model. Excluding the oldest point at ~230cm depth, all non-outlier points are intercepted to some degree by the age depth model.

Elemental ratios without meaningful Itrax and grainsize relationships were omitted. Grainsize range was reduced from 15.216µm to 338.33µm including LA009/17 to 15.216µm to 181.274µm excluding LA009/17. Itrax range was also reduced for all graphs after excluding LA009/17. LA009/17 included the lowest values for Al/Si, K/Si and Ni/Si and included the highest value for Mg/Fe. Mg/Fe had a positive trend line, all others were negative. K/Si had a higher $R^2$ without the upper core, all other $R^2$ values decreased. Al/Si only had a difference in $R^2$ of 0.0153. A correlation matrix (fig.5) was created for Itrax data graphed in figure 5. Al/Si, K/Si and Ni/Si showed high degrees of correlation. To avoid redundant analysis, Ni/Si and K/Si shall be omitted from further examination, as their $R^2$ values are less than that of Al/Si.

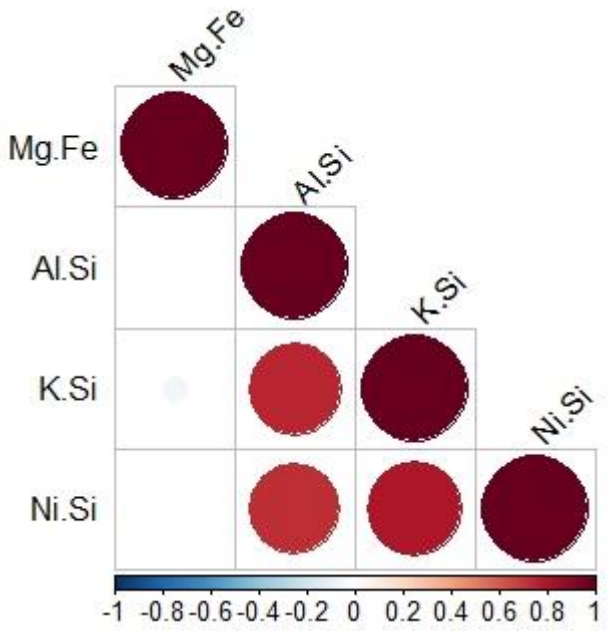


**Figure 5. A correlation matrix for Itrax data created in R. Colour and size of a circle indicates the strength of correlation between data. Data against itself will produce a correlation value of 1.**

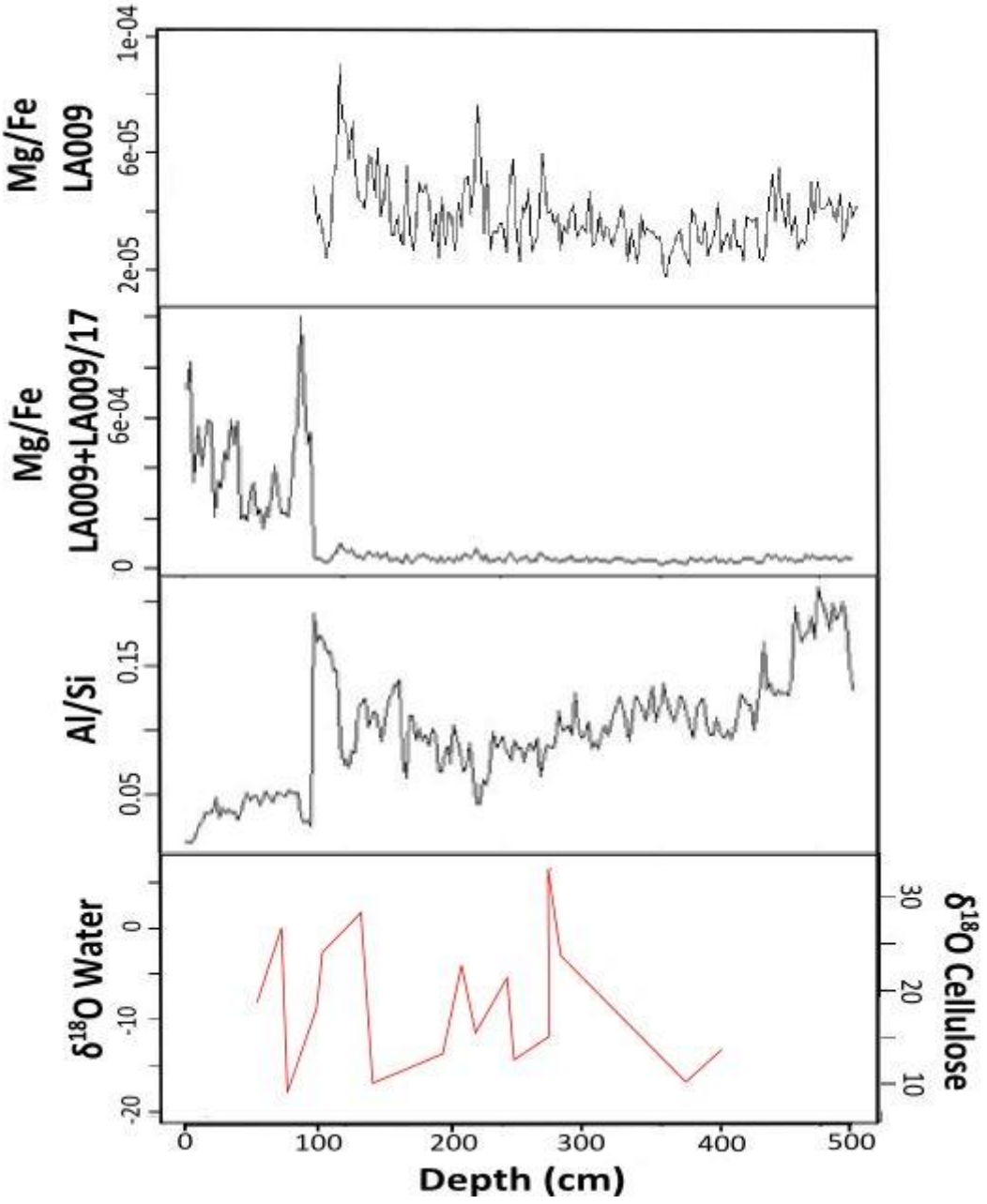


**Figure 6. Al/Si versus age for the lower core section of LA009. Wimmera salinity (Kemp, Radke, Olley, Juggins, & De Deckker, 2012). Mg/Ca taken from bivalves in Blue Lake, South Australia (Gouramanis, Wilkins, & Deckker, 2010). Lake Keilambete water levels inferred from percentage of clay in sediments (Gingele, De Deckker, & Norman, 2007). Al/Si, Salinity and Mg/Ca can be considered inversely proportional to lake/precipitation levels.**

$^{18}O_{water}$ ranges from -20.5 at 62cm depth to 6.54 at 241cm depth. The same depths record $\delta^{18}O_{Cellulose}$ values of 6.47 and 32.83, respectively. The margin of error is 0.411 for all $\delta^{18}O_{Water}$ values and is 0.4 for $\delta^{18}O_{Cellulose}$. $\delta^{18}O$ exhibits no trend but has variability considerably greater than the margin of error. Mg/Fe (LA009+LA009/17)

displays values between 0 and 0.001, whilst Mg/Fe(LA009) has all values lower than 0.0001. There is no trend for Mg/Fe(LA009) however there is a high degree of variance. An abrupt change in values occurs between LA009 and LA009/17 for Mg/Fe and Al/Si.

Mg/Fe increases by an order of magnitude. No trend exists for the LA009/17 section of Mg/Fe but there is again, a high degree of variance. The LA009 section of Al/Si shows an approximate parabolic trend, with values reaching0.2 at 480cm depth and 0.19 at

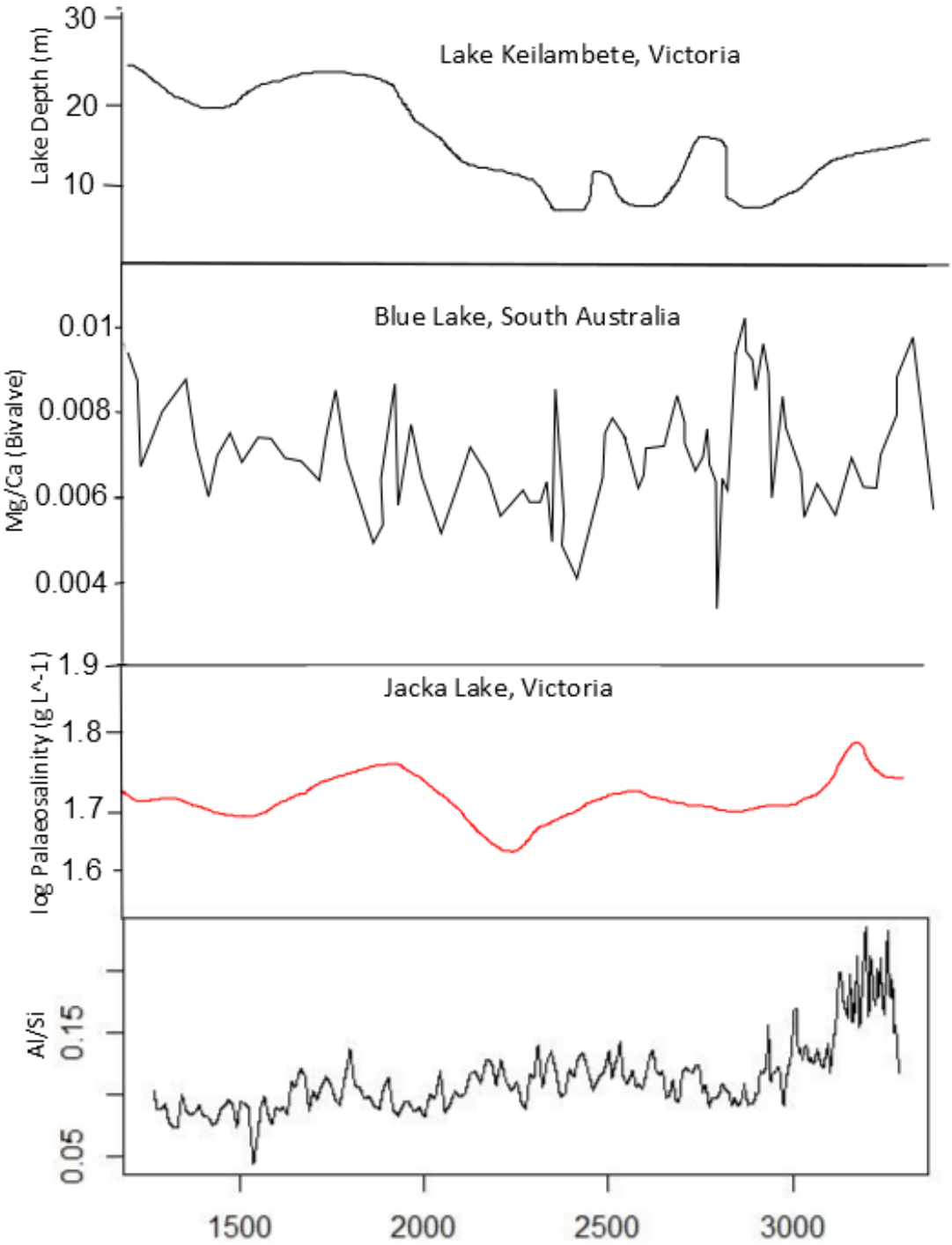


**Figure 7. Al/Si versus age for the lower core section of LA009. Wimmera salinity (Kemp, Radke, Olley, Juggins, & De Deckker, 2012). Mg/Ca taken from bivalves in Blue Lake, South Australia (Gouramanis, Wilkins, & Deckker, 2010). Lake Keilambete water levels infer**

101cm depth. Values dip beneath 0.05 between these points however 0.05 represents the highest values for the LA009/17 section. High Al/Si values between 100 and 120cm appear to correlate with high $\delta^{18}O$ and low Mg/Fe for the LA009 section. Due to the abrupt and sever change in values between LA009 and LA009/17, the two will not be considered part of the same stratigraphy. All Itrax versus depth data can be found in appendix F.

The >0.2 Al/Si region prior to 3.0Ka, seen in fig. 7, correlates to the ~1.8 salinity peak for Jacka Lake and the ~0.01 Mg/Ca peak for Blue Lake at similar ages. Al/Si shows a peak just prior to 3.0Ka at ~0.15 followed by a dip to 0.10 after 3.0Ka and another peak approaching 0.15. Whilst not proportional, this series of features bear a temporily offset resemblance to those seen in Mg/Ca for Blue Lake after 3.0Ka. The general decrease in Al/Si towards the present somewhat corresponds to increasing water levels in Lake Keilambete. Mg/Ca, log palaeosalinity and Al/Si can be considered inversely proportional to meteoric water levels.

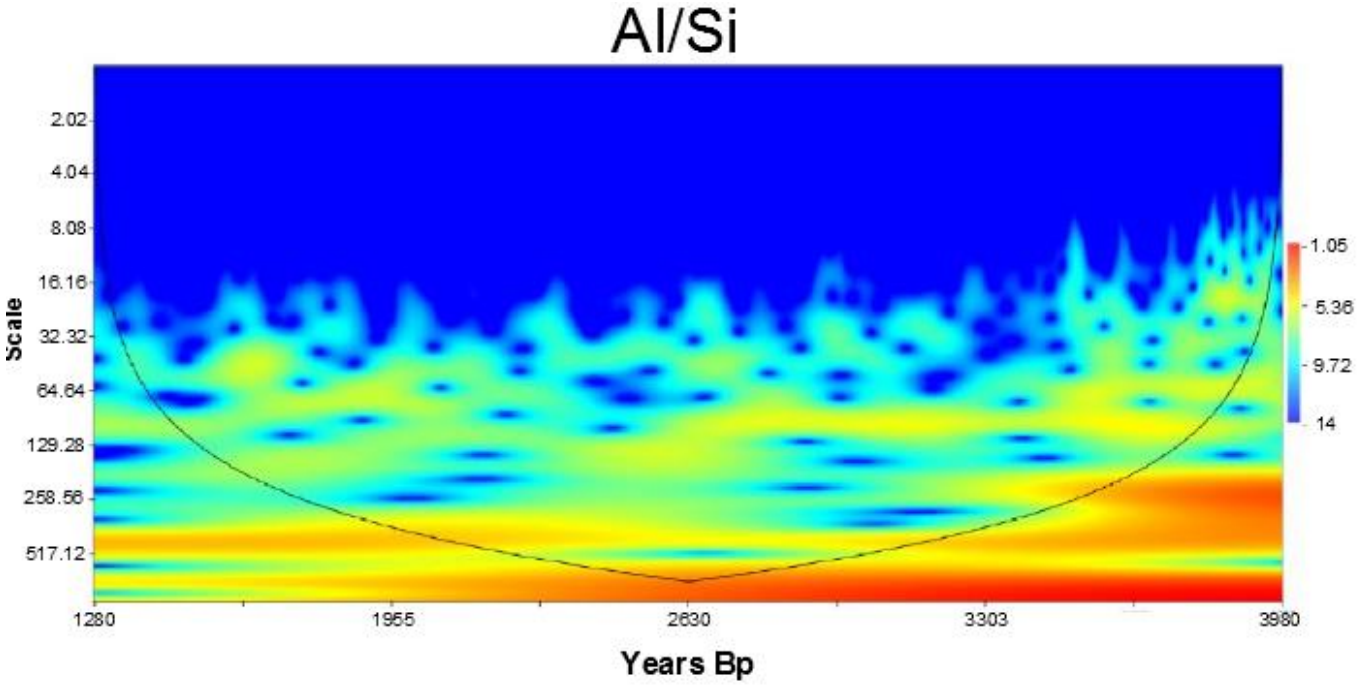


**Figure 8. A continuous wavelet analysis using morelt waves for Al/Si versus years Bp. Wavelet coefficient (scale on the right) represent the strength of 'scale', comparable to the strength of a frequency with correlating wavelengths. High wavelet coefficients indicate higher scale strength. The black line represent the cone of influence, data outside this cone is unusable.**

Baseline wavelet coefficients occur up until ~16.16 scale for all years. Patches of wavelet coefficients reaching up to ~5 present for all years up until ~64 scale. Below this area areas of comparable wavelet coefficients begin to stretch laterally along the time scale. The longest area of elevated wavelet coefficient in this reaches streches from the right edge of the cone of influence to ~2630 yeaps Bp. The highest wavelet coefficient and longest temporal extent occurs at ~500 scale however, the cone of influence is extremely narrow at this point.

## DISCUSSION

The abrupt changes in Itrax values between LA009 and LA009/17 indicate that the two cores do not represent the same stratigraphy. The ages gathered from each core should therefore be examined independently. Ages gathered from LA009/17 make it hard to be confident that there is any meaningful relationship between age and depth. BACON gave LA009/17 a mean accumulations rate of 0.1 yr/cm. However this result is likely erroneous as BACON does not give results lower than 0.1 yr/cm to ensure sediment age always increases with depth. If this limit were not enforced, LA009/17 would likely have an accumulation rate with either a negative or zero value. In reality there are likely two scenarios which would create such a result. The first being that the core sampled a single depositional event such as a sand bank slumping which would create a thick sediment layer with no age-depth correlation. The Itrax data suggests that this is not the case as certain elemental ratios display distinct peaks rather than a homogenous distribution, which would be expected of an instantaneous deposition. Additionally, there is a distinct shelly layer in LA009/17, reflected by the largest Ca/Si peak. Again, such features are not expected to be present in an instantaneous depositional event. This

implies, the problematic age-depth relationship is a result of old plant matter, from which 14C values were derived, being reworked within the sediment or having significant lag between time of growth and time of burial. Unfortunately this means that the LA009/17 age depth model is of little use.

The mean accumulation rate for LA009 cores is ~0.2cm/yr. However this only reflects sedimentation between *ca* 1268 yr BP and *ca* 3939 yr BP. The combined age depth model of LA009 and LA009/17 may still be of use as it shows a rough analogue for a possible scenario between 1268 yr BP and present, however the two shallowest point are still clear outliers. This age-depth model gives a mean accumulation rate of ~0.1cm/yr. Even if this model is rejected, the sedimentation rate between 1268 yr BP and present would still have had to decrease otherwise the remaining depth would have been produced in nearly half the time.

$^{210}$Pb levels were quite low, despite showing a reliable trend. This may be due to the coarse, sandy nature of the sediments. Lower surface area to volume ratios cause larger particles to adsorb less $^{210}$Pb per volume (J. N. Smith & Walton, 1980). The CFCS $^{210}$Pb and CRS $^{210}$Pb both showed accumulation of 0.157cm/yr and 0.15cm/yr, respectively. It is hard to conclude which model is more reliable without a known age calibration. The appearance of *Pinus* pollen occurs outside the interpolated window and the plutonium spike did not appear as expected. Both CFCS and CRS accumulation rates are higher than that of LA009-LA009/17. This supports the hypothesis of increased sedimentation following European colonisation. Confidence in this hypothesis can be greatly increased if sedimentation rates surrounding the appearance of *Pinus* pollen are gathered. Barnett (1994) observed $^{210}$Pb derived accumulation rates nearly three times higher than $^{14}$C

derived accumulation rates. CRS and CFCS models in this study give accumulations roughly 1.5 times that of $^{14}C$. This may be a result of Barnett (1994) using very few $^{14}C$ ages which makes an inaccurate accumulation model more likely. It is also possible that the difference is a result of lateral heterogeneity in Lake Alexandrina's sedimentation. It has already been established from LA009 and LA009/17 that Lake Alexandrina's sediments are not compositionally homogenous, making it probable that accumulation rate is not homogenous either.

The plutonium results did not appear to reflect any nuclear fallout event. A spike appeared at the 6.5cm mark, however the total Pu concentration was less than 0.025 pg/g. This is substantially lower than would be expected were this peak to represent the 1956 nuclear weapons tests (B. S. Smith et al., 2016). Additionally, the $^{210}Pb$ age depth profiles would indicate this depth represents an age close to 1990 not 1956. There are several possible explanations for this observation. Due to Lake Alexandrina's enormous catchment size one might not expect to see such a peak. The time between precipitation at any area within the MDB and the time said water reaches Lake Alexandrina would vary substantially from site to site. If plutonium fallout were to be deposited roughly evenly throughout the catchment, plutonium-bearing sediments would be slowly deposited, region by region. This would mask any peak a plutonium fallout event would create. The general increase in plutonium could be seen to support this argument. A second scenario is that remobilisation of sediment has taken place, either carrying plutonium-bearing sediments elsewhere or homogenising sediments. The lower than expected plutonium levels support this argument. If this is the case however, one would not expect the $^{210}Pb$ ages to show a coherent trend, which they do. Finally, it is possible

that the fallout peak does not occur in the sampled sediment layers. If peak fallout deposition occurred between 10-15cm it is possible that the peak was simply not observed. However, a more obvious tail would still be expected and $^{210}Pb$ ages would not suggest a fallout peak at these depths. Additionally, for reasons stated when discussing the effects of catchment size, an abrupt, narrow peak hidden in unmeasured depths would not be expected of this core. Large catchment size appears to be the most robust explanation for the observed plutonium trends.

The scatter of $\delta^{18}O$ suggests the hydrology of Lake Alexandrina has varied through time. Whilst fluctuations are present, the stationary nature of the data indicates no significant hydrological regime changes have been captured. This is consistent with the notion that the formation of the younghusband peninsula resulted in stable conditions within Lake Alexandrina (Barnett, 1994; Fluin et al., 2009). The data gives an average $\delta^{18}O_{Water}$ of -8.24488. The $\delta^{18}O$ of seawater in South Australia is approximately 0.5 (LeGrande & Schmidt, 2006). Thus the data strongly supports a predominately fresh water regime for the observed period in Lake Alexandrina. It is still possible however, that seawater incursion caused periods of increased $\delta^{18}O$ rather than evaporation as the two effects are indistinguishable without corresponding $\delta^{2}H$ values (Craig, 1961).

Many samples were significantly contaminated. Fourier transform infra-red spectra revealed peaks similar to those of raw clay, as described by S. Louati (2016). With significant peaks at 1644, 1032,798, 778. Pure clay should not affect $\delta^{18}O$ results as clay would be destroyed prior to measurement. Organic material is known to adsorb to clay particles (M. Rebhun, 1992). Samples were treated with sodium chlorite to remove

organics, however it is possible that organics trapped between sheets of clay survived this step and affected $\delta^{18}O$ results. A more significant issue is that contamination would make the measured weight higher than the true weight of cellulose within a sample. As samples were matched with data through weight and peak area, contamination would make it probable that data points show incorrect depths. For this reason, no time series analysis will be conducted for $\delta^{18}O$.

As Al/Si is inversely proportional to grainsize, we can deduce a plausible mechanism where periods of high flow are able to mobilise course, quartz rich particles and periods of low flow allow fine clay particles to fall from suspension. The proportional relationship between Mg/Fe and grainsize suggests a similar mechanism where larger, heavy grains of iron rich minerals such as hematite and magnetite are mobilised during high flow.

Lake Alexandrina's Al/Si, Blue Lake's Bivalve Mg/Ca and Wimmera's salinity all indicate a low water level event between 3.5Ka and 4.0Ka. This indicates a region wide climatic event within south east Australia during this period. The reduction in frequency of moisture rich winds venturing southward is cited as the source of shifts towards aridity during this time for other sites (Gouramanis et al., 2013; Marx et al., 2011). This may explain the observed dry period, however only in Lake Alexandrina do conditions get wetter after this period. Additionally, the notion that ~2Ka represents the driest period for the region is not supported by Al/Si.

Due to having the highest $R^2$ and its correlation to other proxies from lacustrine sites in the same region, Al/Si has been chosen for wavelet analysis. The results of which can be seen in figure 8. No trends in the decadal scale appear, meaning cycles usually cited

as drivers for River Murray flow, such as IOD, IPO and ENSO have not been captured. Strong correlations to climatic cycles on these scales have been made for many sites throughout the MDB. If different climatic cycles dominate different sub catchments throughout the MDB as proposed by Ho et al. (2014), the competing signals may drown out one another when amalgamated at the River Murray's terminus. Relatively high wavelet coefficients are shown at roughly the 80 year scale up until ~2630 years BP. The closest matching climatic oscilation is the Gleissberg solar cycle which has a frequency of 87 years (Hathaway & Wilson, 2004). Solar cycles can affect rainfall or lack thereof, as changes in solar activity affects earth's temperature which could affect atmospheric and hydrological activity. There is no mention of the Gleissberg solar cycle influencing sites across the MDB and south east Australia. However, an 87 year cycle could easily go undetected using only observational data and paleo time series analysis in the region is lacking. The signal is mild enough that noise within the data could plausibly produce such a result, however. Similar analysis for sites within south east Australia and the MDB could help to decipher whether the Gleissberg cycle has ever had a significant effect in the region. Wavelet analysis on other environmental proxies in Lake Alexandrina could also aid in a similar manner. The strongest signal appears at the ~500 year scale. However the cone of influence at this scale is not much longer than 500 years itself, meaning that any roughly parabolic trend stretching through this time would be interpreted as a signal. It is also generally a red flag when the most intense frequency is the largest as noise over long scales may be interpreted as oscilation by a wavelet.

## CONCLUSIONS

Differences in sediment accumulation rates between $^{210}$Pb and $^{14}$C chronologies support the hypothesis of anthropogenic, increased sedimentation rate following European colonisation. The difference between $^{210}$Pb derived accumulation and $^{14}$C derived accumulation is not consistent with other studies, however. This is unsurprising as the contrasting sediments of LA009 and LA009/17 highlight the potential lateral heterogeneity within lakes. This should be taken into account in further lacustrine studies as one should be aware that a single lake can produce different stratigraphies even within a small area. Improved $^{210}$Pb accumulation rates around the appearance of *Pinus* pollen could be used to strengthen the notion that differences in $^{14}$C accumulation and $^{210}$Pb are a result of European colonisation.

$\delta^{18}$O supports a predominately freshwater history for Lake Alexandrina, however periods of seawater incursion are still possible. The degree of variance in $\delta^{18}$O appears relatively constant throughout time indicating the drivers of high and low $\delta^{18}$O values have been present for at least the past 3980 years BP. Obtaining $\delta^{2}$H for the sight can help resolve whether variation in $\delta^{18}$O is evaporative or seawater driven.

Certain peaks in $\delta^{18}$O appear to correlate with Al/Si. Additionally, some climatic events from sites throughout south east Australia line up with similar climatic events captured by Al/Si in Lake Alexandrina. A dry period between 4.0Ka and 3.5Ka was observed in Blue Lkae, Jacka Lake and Lake Alexandrina. These correlations, alongside the highly plausible mechanism ofcoarse quartz grains being deposited during high flow and finer clay particles falling out of suspension during low flow, indicate that Al/Si is a

meaningful proxy in Lake Alexandrina. This gives precedent for similar approaches in other study sites when high resolution data is desirable.

Wavelet analysis revealed the Gleissberg potentially having an effect on Lake Alexandrina's hydrology up until ~2630 years BP. This is a novel result for sites within south east Australia and the Murray-Darling Basin. Similar time series analysis on lakes throughout the region would help make these assertions more robust.

## ACKNOWLEDGMENTS

Acknowledgements and thank go out to:
ANSTO
Atun Zawadzki
David Child
Fiona Bertuch
Haidee Cadd
Tiah Bampton
Tony Hall
Robert Klaebe
Chloe Dean
Kalimna Roe-Simons
Isaac Axford

## REFERENCES

APPLEBY, P. G., & OLDFIELD, F. 1978. The calculation of lead-210 dates assuming a constant rate of supply of unsupported 210Pb to the sediment. *Catena*, ***5***(1), 1-8.

AULT, T. R., COLE, J. E., OVERPECK, J. T., PEDERSON, G. T., ST. GEORGE, S., OTTO-BLIESNER, B., DESER, C. 2014. The Continuum of Hydroclimate Variability in Western North America during the Last Millenium. *American Meteorological Society*, ***26***, 5863-5878.

BARNETT, E. J. 1994. A Holocene paleoenvironmental history of Lake Alexandrina, South Australia. *Journal of Paleolimnology, **12***(3), 259-268.

BIRKS, S. J., EDWARDS, T. W. D., & REMENDA, V. H. 2007. Isotopic evolution of Glacial Lake Agassiz: new insights from cellulose and porewater isotopic archives. *Palaeogeography, Palaeoclimatology, palaeoecology*, ***246***, 8-22.

BLAAUW, M., & CHRISTEN, J. A. 2011. Flexible paleoclimate age-depth models using an autoregressive gamma process. *Bayesian Analysis, **6***, 457-474.

BOURMAN, R. P., & BARNETT, E. J. 1996. Impacts of river regulation on the terminal lakes and mouth of the River Murray, South Australia. *Oceanographic Literature Review, **43***(2), 196.

BOURNMAN, R. P., MURRAY-WALLACE, C. V., BELPERIO, A. P., & HARVEY, N. 2000. Rapid coastal geomorphic change in the River Murray Estuary of Australia. *Marine Geology, **170***(1-2), 141-168.

*Climate Change 2007 - Impacts, Adaption and Vulnerability*. 2007. Cambridge Cambridge University Press, 2007.

CRAIG, H. (1961). Isotopic Variations in Meteoric Waters. *Science, 133*(3465), 1702-1703.

DENIRO, M. J., & EPSTEIN, S. 1981. Isotopic composition of cellulose from aquatic organisms. *Geochemica et Cosmochimica Acta, **45***, 1885-1894.

EDWARDS, T. W. D., & MCANDREWS, J. H. 1989. Paleohydrology of a Canadian Shield lake inferred from 18O in sediment cellulose. *Canadian Journal of Earth Sciecnes, **26***(9), 1850-1859.

EPSTEIN, S., P., T., & YAPP, C. J. 1977. Oxygen and hydrogen isotopic ratios in plant cellulose. *Science, **198***, 1209-1215.

FLUIN, J., GELL, P., HAYNES, D., TIBBY, J., & HANCOCK, G. 2007. Palaeolimnological evidence fot the independent evolution of neighbouring terminal lakes, the Murray Darling Basin, Australia. *Hydrobiologia, **591***(117-134).

FLUIN, J., HAYNES, D., & TIBBY, J. 2009. An Environmental History of the Lower Lakes and the Coorong. In D. H. Jennie Fluin, John Tibby (Ed.): Government of South Australia

GELL, P., FLUIN, J., TIBBY, J., HANCOCK, G., HARRISON, J., ZAWADZKI, A., WALSH, B. 2009. Anthropogenic acceleration of sediment accrestion in lowland floodplain wetlands, Murray-Darling Basin, Australia. *Geomorphology, **108***(1-2), 122-126.

GELL, P., TIBBY, J., BALDWIN, D., & HANCOCK, G. 2007. The impact of regulation and salinisation on floodplain lakes: the lower River Murray, Australia. *Hydrobiologia, **591***, 135-146.

GINGELE, F., DE DECKKER, P., & NORMAN, M. 2007. Late Pleistocene and Holocene climate of SE Australia reconstructed from dust and river loads deposited offshore the rIver Murray Mouth. *Earth and Planetary Science Letters, **255***, 257-272.

GOURAMANIS, C., DE DECKKER, P., SWITZER, A. D., & WILKINS, D. 2013. Cross-continent comparison of high-resolution Holocene climate records from souther Australia - Deciphering the impacts of far-field teleconnections. *Earth-Science reviews, **121***, 55-72.

GOURAMANIS, C., WILKINS, D., & DECKKER, P. 2010. 6000 years of environmental changes recorded in Blue Lake, South Australia, based on ostracod ecology and valve chemistry. *Palaeogeography, Palaeoclimatology, palaeoecology, **297***, 223-237.

HALLEGATTE, S., GREEN, C., NICHOLLS, R. J., & CORFEE-MORLOT, J. 2013. Future flood losses in major coastal cities. *national climate change, **3***, 802-806.

HAMMER, O., DAVID, A. T., HARPER, D. A. T., & RYAN, P. D. 2001. PAST: Paleontological statistics software package for education and data analysis. *Palaeontological Association*.

HATHAWAY, D. H., & WILSON, R. M. 2004. What the Sunspot Record Tells Us About Space Climate. *Solar Physics, **224***(1-2), 5-19.

HAU, Q., BARBETTI, M., JACOBSEN, G. E., ZOPPU, U., & LAWSON, E. M. 2000. Bomb radiocarbon in annual tree rings drom Thailand and Australia. *Nuclear Instruments and Methods in Physics Research, **72***, 359-365.

HO, M., VERDON-KIDD, D. C., & KIEM, A. S. 2014. Broadening the Spatial Applicability of Paleoclimate Information - A Case Study for the Murray-Darling Basin, Australia. *Journal of Climate, **27***, 2477-2495.

HOTCHKIS, M. A. C., CHILD, D. P., FROEHLICH, M. B., WALLNER, A., WILCKEN, K., & WILLIAMS, M. 2019. Actinides AMS on the VEGA accelerator. *Nuclear Instruments and Methods in Physics Research B, **438***(70-76).

HUGHES, C. E., & CRAWFORD, J. 2012. A new precipitation weighted method for determining the meteoric water line for hydrological applications demonstrated using Australian and global GNIP data. *Journal of Hydrology, **464-465***, 344-351.

KEMP, J., RADKE, L. C., OLLEY, J., JUGGINS, S., & DE DECKKER, P. 2012. Holocene lake salinity chnages in the Wimmera, southeastern Australia, provide evidence for millenial-scale climate variability *Quaternary Research, **77***, 65-76.

LI, Y., GUO, Y., & YU, G. 2013. An analysis of extreme flood events during the past 400 years at Taihu Lak, China. *Journal of Hydrology, **500***, 217-225.

LEGRANDE, A. N., & SCHMIDT, G. A. 2006. Global gridded data set of the oxygen isotopic composition in seawater. *Geophysical Research Letters, **33***(12).

M. REBHUN, R. K., L. GROSSMAN, J. MANKA, C. H. RAV-ACHA. 1992. Sorption of Organics on Clay and Synthetic Humic-Clay Complexes Simulating Aquifer Processes. *Water Research, **26***(1), 79-84.

MACDONALD, G. M., EDWARDS, T. W. D., MOSER, K. A., PIENITZ, R., & SMOL, J. P. 1993. Rapid response of treeline vegetation and lakes too past climate warning *Nature, **361***, 243-246.

MACDONALD, N., KJELDSEN, R. R., PROSDOCIMI, I., & SANGSTER, H. 2014. Reassessing flood frequency for the Sussex Ouse, Lewes: the inclusion of historical flood information since AD 1650. *Natural Hazards and Earth System Sciences, **14**,* 2817-2828.

MARX, S. K., KAMBER, B. S., MCGOWAN, H. A., & DENHOLM, J. 2011. Holocene dust deposition rates in Australia's Murray-Darling Basin record the interplay between aridity and the position of the mid-latitude westerlies. *Quaternary Science Reviews, **30***(23-24), 3290-3305.

S. LOUATI, S. B., B. SAMET. 2016. Geopolymers Based on Phosphoric Acid and Illito-Koalinitic Clay. *Advances in Materials Science and Engineering, 2016*.

SIMPSON, H. J., CANE, M. A., HERCZEG, A. L., ZEBIAK, S. E., & SIMPSON, J. H. 1993. Annual river discharge in southeastern Australia related to El Nino-Southern Oscillation forecasts of sea surface temperatures *Water Resources Research, **29***(11), 3671-3680.

SKINNER, L. C., & MCCAVE, I. N. 2003. Analysis and modelling of gravity- and piston coring based on soil mechanics. *Marine Geology, **199***(1-2), 181-204.

SMITH, B. S., CHILD, D. P., FIERRO, D., HARRISON, J. J., HEIJNIS, H., HOTCHKIS, M. A. C., ZAWADZKI, A. 2016. Measurement of fallout radionuclides, 239, 240 Pu and 137 Cs, in soil and creek sediment: Sydney Basin, Australia. *Journal of Environmental Radioactivity, **151***(3), 579-586.

SMITH, J. N., & WALTON, A. 1980. Sediment accumulation rates and geochronologies measured in the Saguenay Fjord using the 210Pb dating method. *Geochemica et Cosmochimica Acta, **44***, 225-240.

STEPHENSON, A. E., & BROWN, C. M. 1989. *Geology of the Murray Basin, southeastern Australia, Groundwater Series 17*.

THORNDYCRAFT, V., HU, Y., OLDFIELD, F., CROOKS, P.R.J., & APPLEBY, P.G. 1998. Individual flood events detected in the recent sediments of the Petit Lac d'Annecy, eastern France. *The Holocene, **8***(6), 12-20

TUNIZ, C., FINK, D., HOTCHKIS, M. A. C., JACOBSEN, G. E., LAWSON, E. M., SMITH, A. M., BOLDEMAN, J. W. 1994. The ANTARES AMS Centre at the Lucas Heights Research Laboratories. *Nuclear Instruments and Methods in Physics Research**, 92***, 22.

VANDEPUTTE, K., MOENS, L., & DAMS, R. 1996. Improved sealed-tube combustion of organic samples to CO2 for stable isotopic analysis, radiocarbon dating and percent carbon determinations. *Analytical Letters, **29***(15), 1761-2773.

VOGEL, J. S., SOUTHON, J. R., NELSON, D. E., & BROWN, T. A. 1984. Performance of catalytically condensed carbon for use in Accelerator Mass Spectrometry. *Nuclear Instruments and Methods in Physics Research, **5,*** 289-293.

WALKER, K. 2006. Serial weirs, cumulative effectsL the Lower River Murray, Australia. In R. Kingsford (Ed.), *Ecology of Desert Rivers* (pp. 248-279). Cambridge, Uk: Cambridge University Press.

WALKER, K. F. 1985. A review of the ecological effects of river regulation in Australia. *Perspectives in SOuthern Hemisphere Limnology, **125***, 111-129.

WISSEL, H., MAYR, C., & LUCKE, A. 2008. A new approach for the isolation of cellulose from aquatic plant tissue and freshwater sediments for stable isotope analysis. *Organic Geochemistry, **39***, 1545-1561.

WOLFE, B. B., EDWARDS, T. W. D., ARAVENA, R., FORMAN, S. L., WARNER, B. G., A.A., V., & MACDONALD, G. M. 2000. Holocene paleohydrology and paleoclimate at treeline, north-central Russia, inferred from oxygen isotope records in lake sediment cellulose. *Quaternary Research, **53***, 319-329.

WOLFE, B. B., KARST-RIDDOCH, T. L., VARDY, S. R., FALCONE, M. D., HALL, R. I., & EDWARDS, T. W. D. 2005. Impacts of climate, river flooding on the hydro-ecology of a floodplain basin, Paece-Athabasca Delta, Canada since A.D 1700. *Quaternary Research, **64***, 147-162.

YAKIR, D., & DENIRO, M. 1990. Oxygen and Hydrogen Isotope Fractionation during Cellulose Metabolism in Lemma gibba L.*Plant Physiology, **93***, 325-332.

**APPENDIX A: CAS CHEMISTRY – PROCESSING RADIOCARBON SAMPLES**

# Purpose

To establish a standard instruction for the processing of samples that have been pre-treated, and require isolation of carbon and conversion to a form suitable for radiocarbon dating.

# Scope

The requirements of this instruction shall apply to processing of radiocarbon samples for the purpose of radiocarbon dating using accelerator mass spectrometry

## Table of Contents

# 1. Conversion to $CO_2$

## 1.1. Organic samples

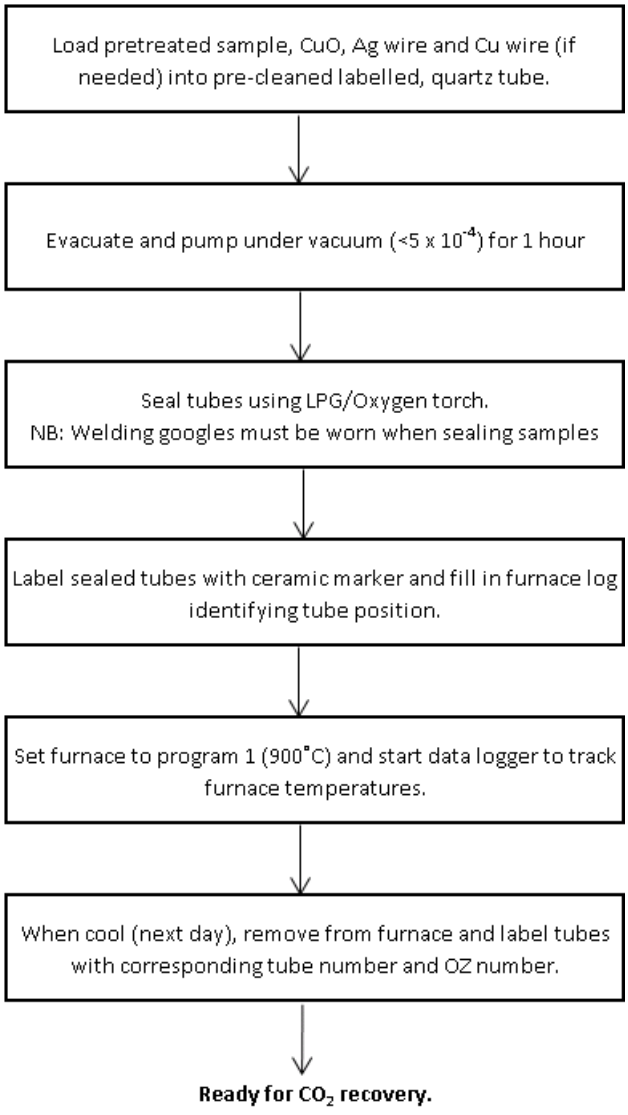

## 1.2. Carbonate samples

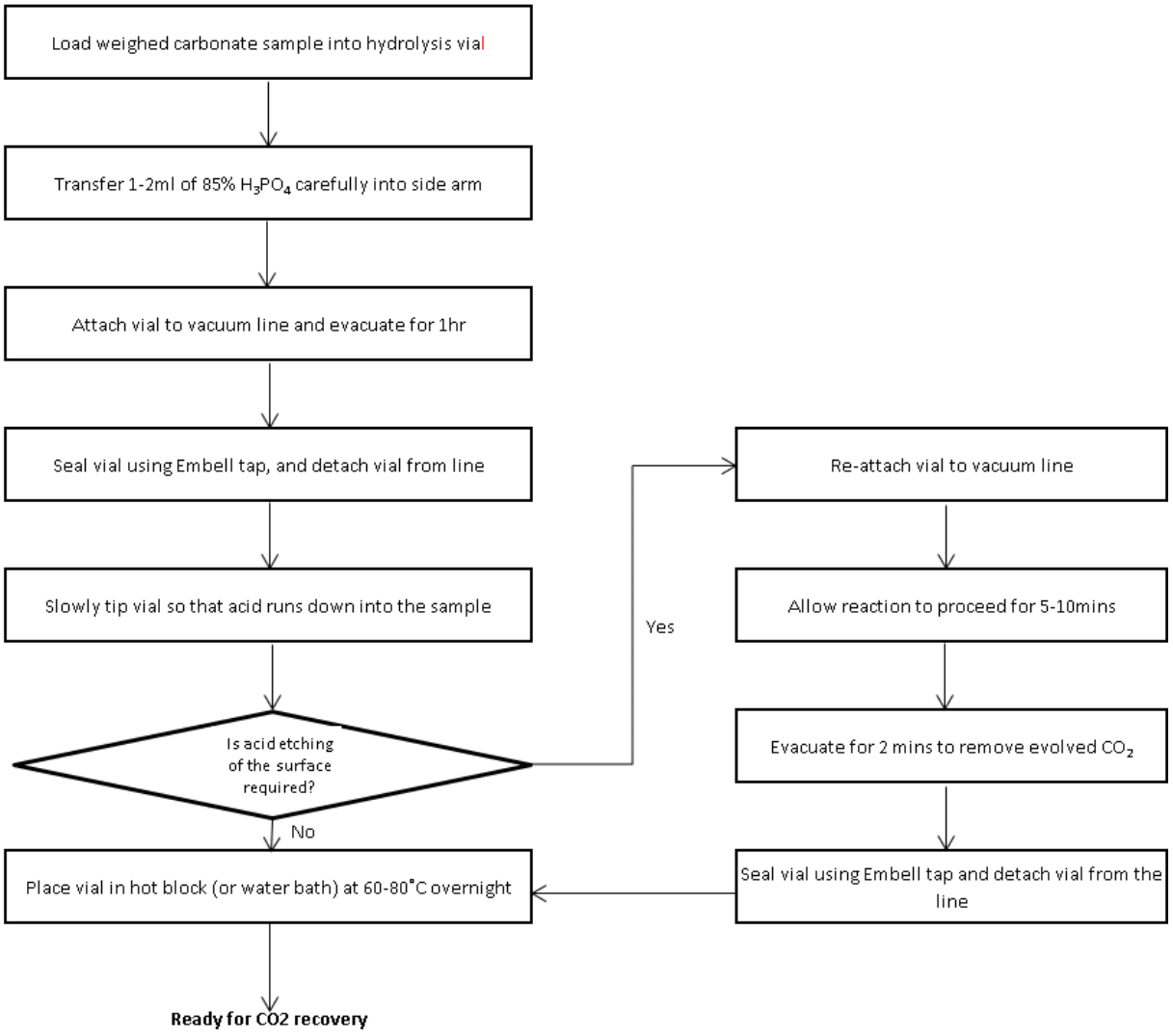

## 1.3. Hydrolysis of Dissolved Inorganic Carbon (DIC) in waters

### 1.3.1. $N_2$ Glove box

The volume of water required should be calculated from the carbonate content of the water (if supplied). Groundwaters should be filtered prior to processing; this should be done in a glove box under a nitrogen atmosphere, using the Millipore ® Filter Unit.

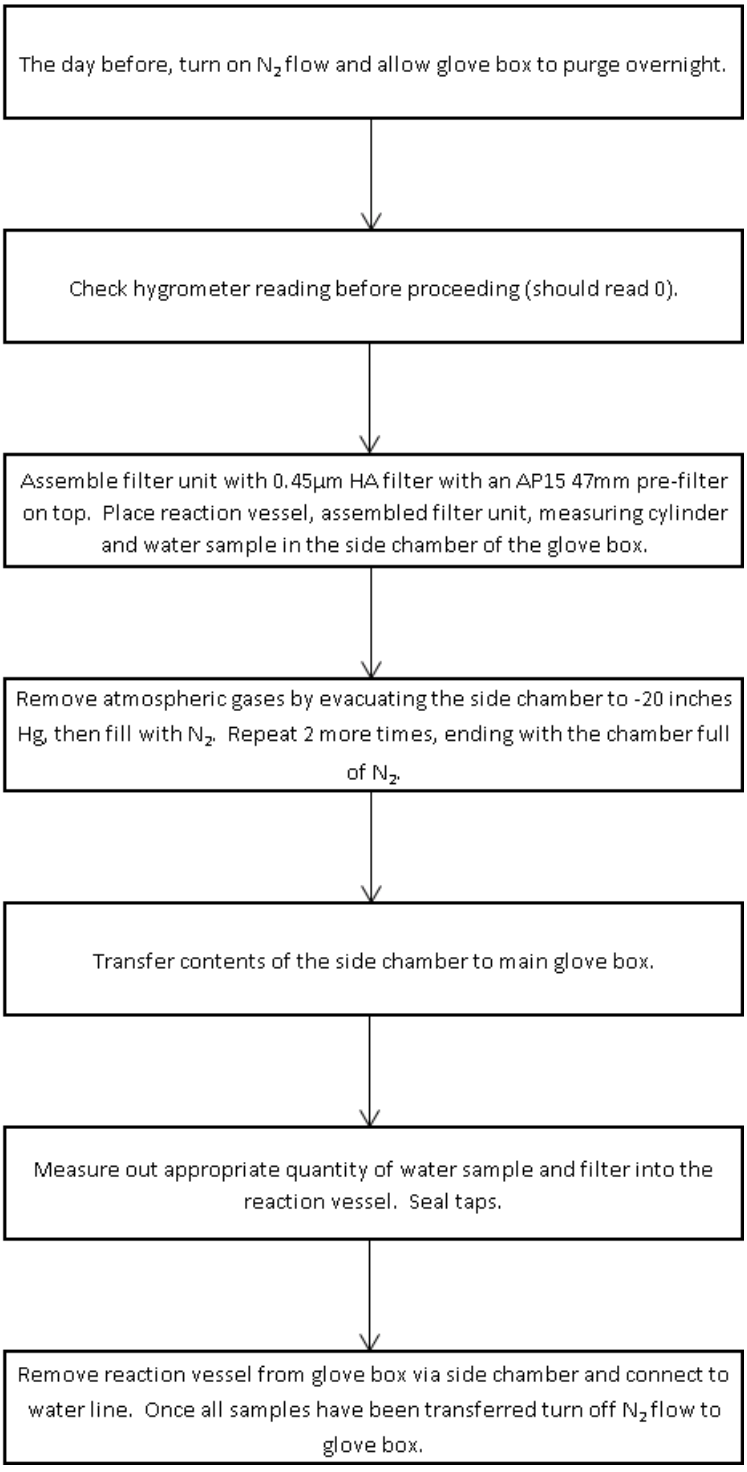

### 1.3.2. Water line

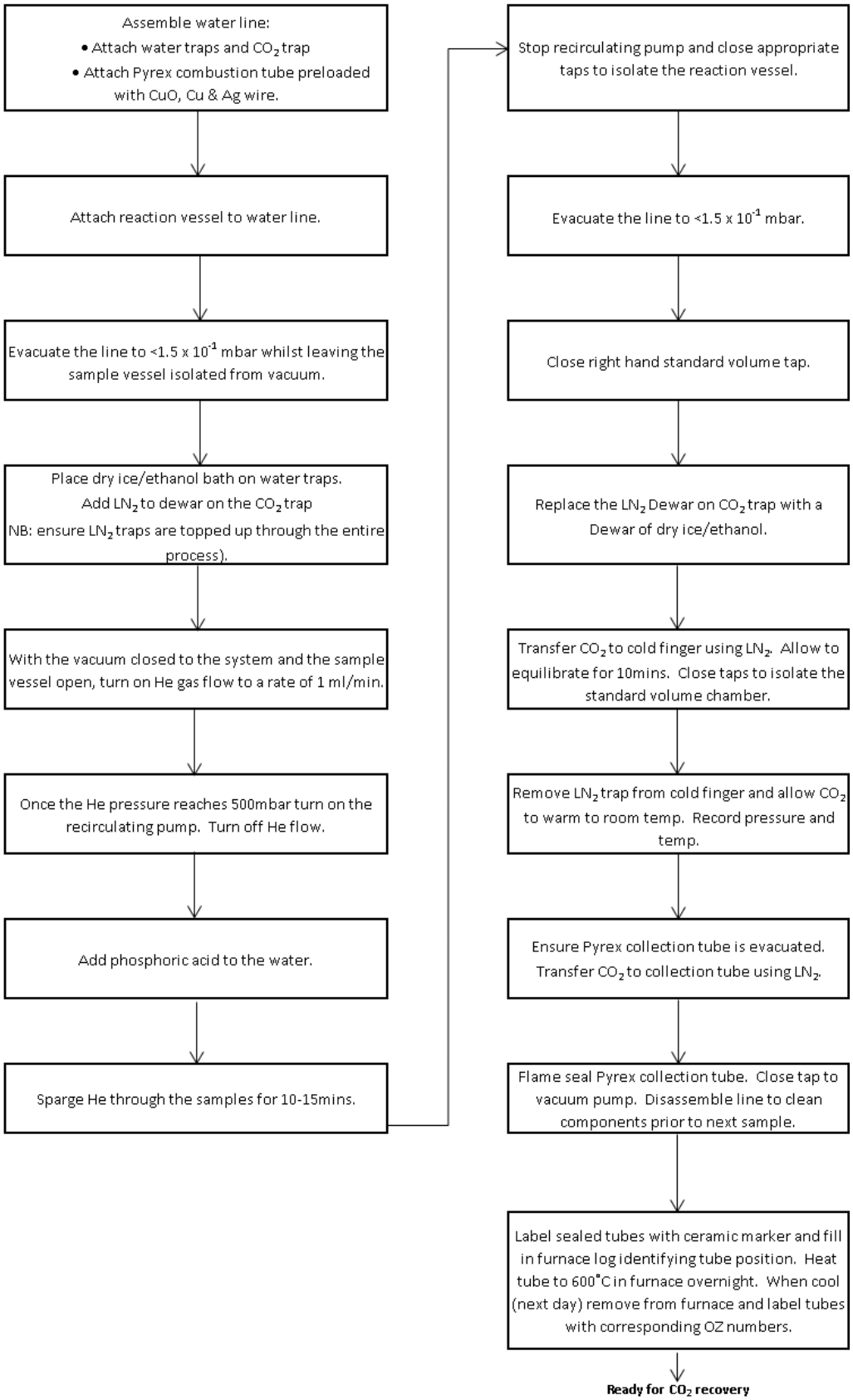

# 2. $CO_2$ recovery and measurement

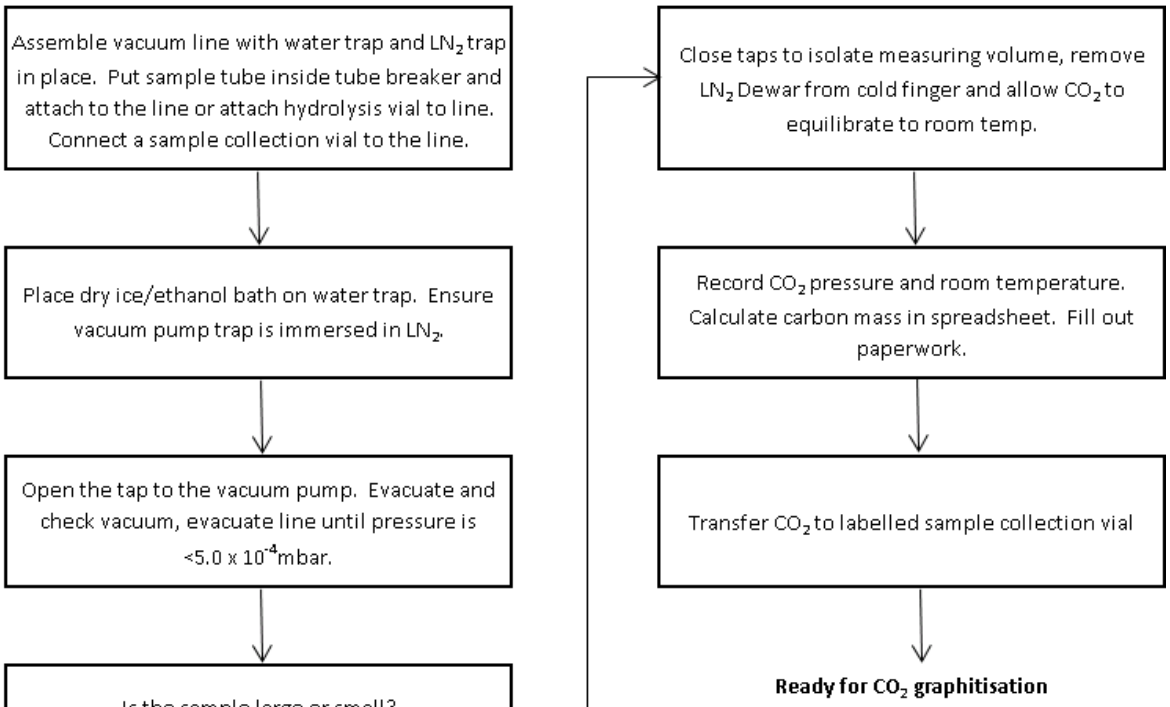
Assemble vacuum line with water trap and $LN_2$ trap in place. Put sample tube inside tube breaker and attach to the line or attach hydrolysis vial to line. Connect a sample collection vial to the line.
Place dry ice/ethanol bath on water trap. Ensure vacuum pump trap is immersed in $LN_2$.
Open the tap to the vacuum pump. Evacuate and check vacuum, evacuate line until pressure is $<5.0 \times 10^{-4}$mbar.
Is the sample large or small?
Large: select large volume measuring chamber (with 1000 torr gauge).
Small: Select small volume measuring chamber (with 10 torr gauge).
Close valve to isolate measuring chamber from the vacuum pump
Place $LN_2$ Dewar on measuring volume cold finger
Break sample tube or open tap on hydrolysis vial and wait for $CO_2$ to collect in cold finger
Evacuate to remove noncondensable gases. Close off vacuum.
Close taps to isolate measuring volume, remove $LN_2$ Dewar from cold finger and allow $CO_2$ to equilibrate to room temp.
Record $CO_2$ pressure and room temperature. Calculate carbon mass in spreadsheet. Fill out paperwork.
Transfer $CO_2$ to labelled sample collection vial
**Ready for $CO_2$ graphitisation**

# 3. $CO_2$ Graphitisation

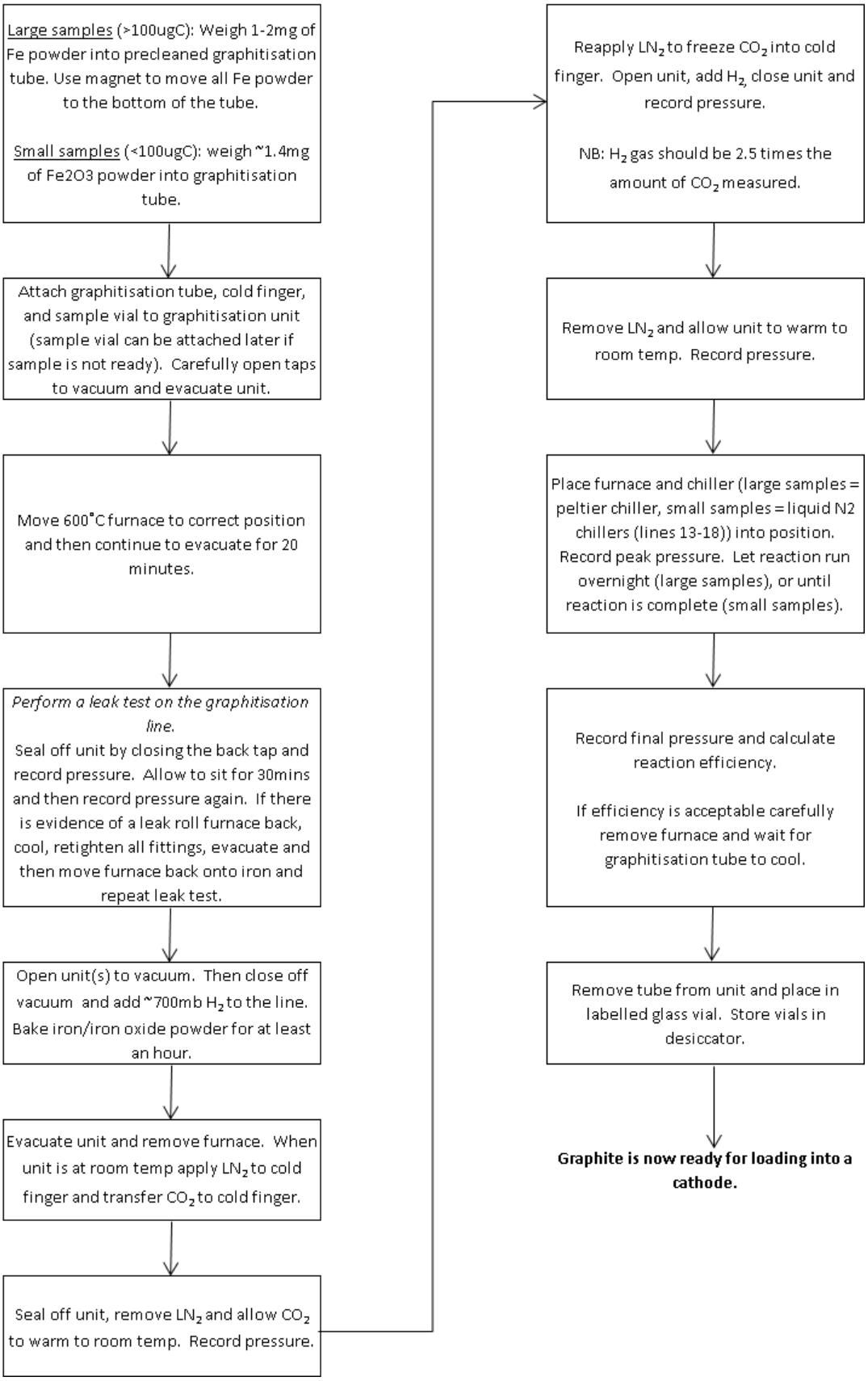
Large samples (>100ugC): Weigh 1-2mg of Fe powder into precleaned graphitisation tube. Use magnet to move all Fe powder to the bottom of the tube.
Small samples (<100ugC): weigh ~1.4mg of Fe2O3 powder into graphitisation tube.
Attach graphitisation tube, cold finger, and sample vial to graphitisation unit (sample vial can be attached later if sample is not ready). Carefully open taps to vacuum and evacuate unit.
Move 600°C furnace to correct position and then continue to evacuate for 20 minutes.
Perform a leak test on the graphitisation line.
Seal off unit by closing the back tap and record pressure. Allow to sit for 30mins and then record pressure again. If there is evidence of a leak roll furnace back, cool, retighten all fittings, evacuate and then move furnace back onto iron and repeat leak test.
Open unit(s) to vacuum. Then close off vacuum and add ~700mb H2 to the line. Bake iron/iron oxide powder for at least an hour.
Evacuate unit and remove furnace. When unit is at room temp apply LN2 to cold finger and transfer CO2 to cold finger.
Seal off unit, remove LN2 and allow CO2 to warm to room temp. Record pressure.
Reapply LN2 to freeze CO2 into cold finger. Open unit, add H2, close unit and record pressure.
NB: H2 gas should be 2.5 times the amount of CO2 measured.
Remove LN2 and allow unit to warm to room temp. Record pressure.
Place furnace and chiller (large samples = peltier chiller, small samples = liquid N2 chillers (lines 13-18)) into position. Record peak pressure. Let reaction run overnight (large samples), or until reaction is complete (small samples).
Record final pressure and calculate reaction efficiency.
If efficiency is acceptable carefully remove furnace and wait for graphitisation tube to cool.
Remove tube from unit and place in labelled glass vial. Store vials in desiccator.
Graphite is now ready for loading into a cathode.

# 4. Cathode loading

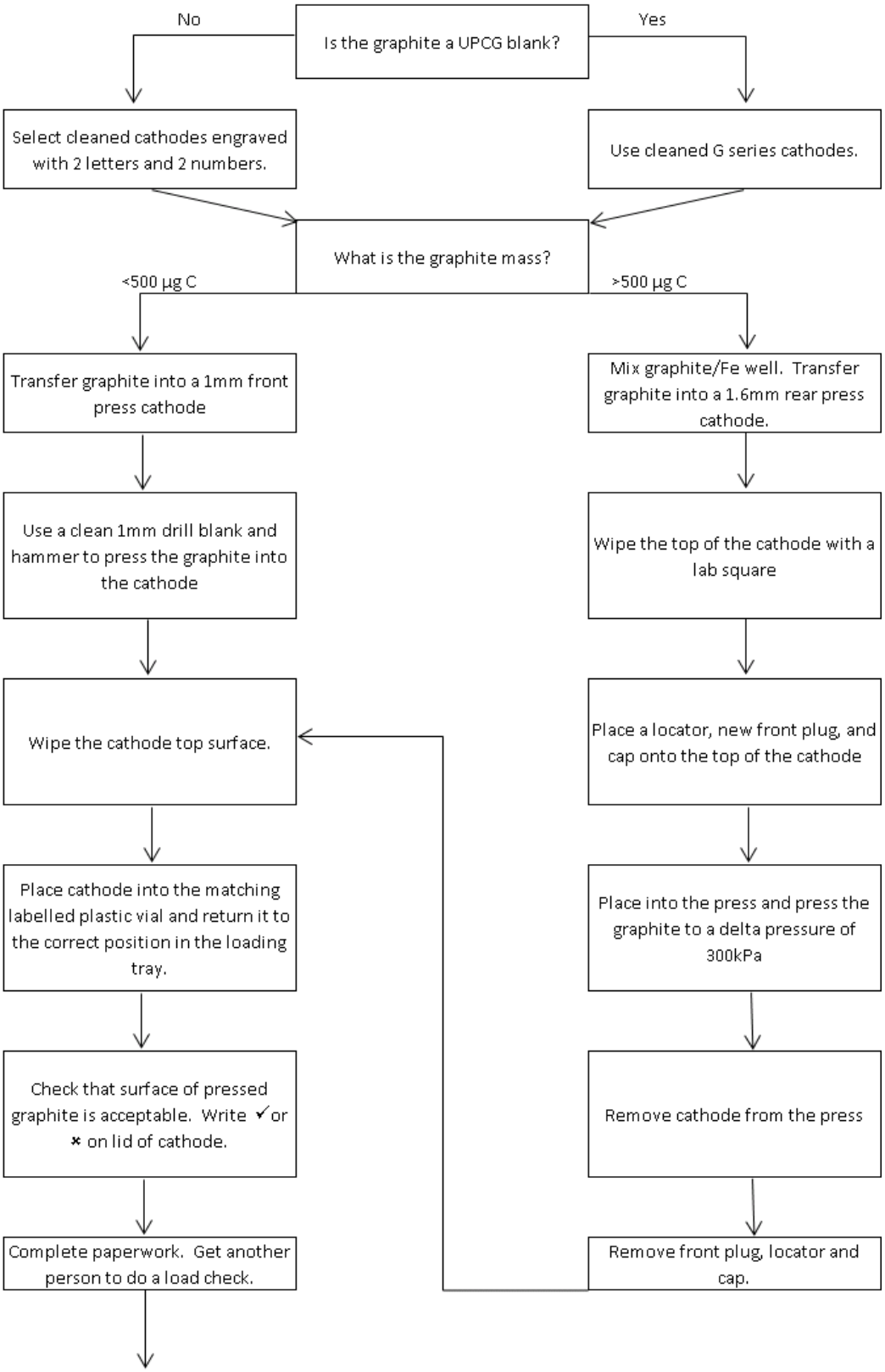


**Sample information is now ready to be put in chemlist and cathode placed in current accelerator run rack.**

# 5. Definitions

| Term | Definition |
|---|---|
| **Milli-RO water** | *Reverse osmosis water processed through a Milli-RO purification unit* |
| **Milli-Q water** | *De-ionised water processed through a Milli-Q purification unit* |
| **DIC** | *Dissolved inorganic carbon* |
| **Graphite** | *A physical form of solid carbon* |
| **Cathode** | *The target holder into which the graphite for AMS measurement is placed* |
| **Pressing Pin** | *The pin inserted from the back of the cathode, which compresses the graphite* |
| **Pressing Plug** | *The flat ended stainless steel plug that the graphite is pressed against* |

# 6. References


- Mook, W.G., and Streurman, H.J., 1983, Physical and chemical aspects of radiocarbon dating*. In*
- Mook, W.G., and Waterbolk, H.T., (eds). *Proceedings of the First International Symposium on 14C*

  *and Archaeology*, 1981, Groningen. PACT 8: 33-35.
- Gagnon, A.R., and Jones, G. A., 1993. AMS-Graphite target production methods at Woods Hole

  Oceanographic Institution during 1986-1991. Radiocarbon 35 (2): 301-310.
- Olsson, R. G., and Turkdogan, E. T., 1974. Catalytic effect of iron on the decomposition of carbon

  monoxide: II. Effect of addition of H2, CO2, SO2 and H2S. Metallurgical Transactions 5:21-26.
- Vandeputte, K., Moens, L., and Dams, R., 1996. Improved sealed-tube combustion of organic

  samples for stable isotope analysis, radiocarbon dating and percent carbon determinations.

  Analytical Letters 29 (15): 2761-2273.
- Jull, A.J.T, D.J. Donnahue, A.L. Hatheway, T.W. Linick and L.J. Toolin. 1986. Production of

  graphite targets by deposition from CO/H2 for precision accelerator 14C measurements.

  Radiocarbon 28 (2A): 191-197.
- McNichol, A.P., A.R. Gagnon, G.A. Jones and E.A. Osborne. 1992. Illumination of a black box:

  Analysis of gas composition during graphite target preparation. Radiocarbon 34 (3): 321-329.
- Verkouteren, R.M., G.A. Klouda, L.A. Currie, D.J. Donahue, A.J.T. Jull and T.W. Linick. 1987.

  Preparation of microgram samples on iron wool for radiocarbon analysis via Accelerator Mass

  Spectrometry: A closed-system approach. Nuclear Instruments and Methods in Physics Research

  B29: 41-44.
- Vogel, J.S., J.R. Southon and D.E. Nelson. 1987. Catalyst and binder effects in the use of

filamentous graphite for AMS. Nuclear Instruments and Methods in Physics Research B29: 50-56.

## APPENDIX B: RADIUM CHEMICAL ISOLATION

# Purpose

This instruction establishes the Isotope Tracing in Natural Sytems (ITNS) requirements for the analysis of radium-226 ($^{226}$Ra), undertaken at ANSTO Environmental Radioactivity Measurement Centre (ERMC).

The instruction explains how $^{226}$Ra is concentrated by co-precipitation, collected on a colloidal precipitate of barium sulphate on a membrane filter and assayed by alpha spectrometry (see Appendix A).

# Scope

This analytical scheme has been designed for the determination of $^{226}$Ra in waters, rocks, soils, sediments and biological material. Since other radionuclides separate during the process, reference to their isolation is included.

## Document History

This instruction replaces the old instruction VI 3330. This is a revision to add extra information on how to prepare all the reagents used in this analytical procedure and more relevant References.

### Table of Contents

# 7. Pre-Requisites

## 7.1. Precautions

1. If multiple elements are being analysed, read all associated instructions to avoid chemical/process incompatibilities.
2. This method relies on the production of a special type of alpha particle source which is composed of a thin colloidal form of $BaSO_4$ evenly distributed onto a smooth-surfaced 0.1 µm Millipore "VV" membrane filter. No other filters are suitable.
3. The diluted, 900 mL aliquot of sample needed for the beginning of this analysis must be < 1 M in acid concentration of the type $HNO_3$ or $HClO_4$ and <0.5 M in HCl which tends to complex lead.
4. It must also contain no more than 0.02 M $Ca^{2+}$ otherwise excessive $CaSO_4$ precipitate will form, which cannot be solubilised with $Na_5DTPA$ (complexing agent). If excess Ca is present in the sample (i.e. check for presence of marine shells ($CaCO_3$)), then radium etc. should have been collected by Manganese Dioxide Co-precipitation (see Reference).
5. If the samples are known to have elevated levels of metal pollution, Manganese Dioxide Co-precipitation (see Reference) should be performed following the polonium auto-deposition step. The solution should then be diluted to 2 to 3 L (instead of 800 mL) to ensure removal of interfering substances by performing a greater dilution.
6. If 50 mg Ba or more is not present in the sample on dissolution, then 500 µg $Ba^{2+}$ must be added (particularly important for water samples). Add barium carrier when preparing blank samples.

Solid samples (soils, rocks, etc.) usually contain sufficient Ba but if it exceeds 1 g, then, this will lead to a $BaSO_4$ alpha source that may be too thick.

7. If the analysis sequence follows on from a polonium chemical isolation (see Reference) then the solution is diluted to 800 mL with reagent water and the process begins at step 7 (in section 2. Instructions).

## 7.2. Responsibility

1. The analyst shall be responsible for:
   a. performing all operations in a safe manner, see the ERMC Safety Assurance Committee (SAC) form (see Reference),
   b. applying the best quantitative practices in handling/transferring solutions,
   c. ensuring all apparatus is cleared away and stored on completion of analysis,
   d. recording any difficulties with or changes to this instruction on the corresponding Radium-226 analysis data sheet (Appendix B).

## 7.3. Apparatus and Materials

- 1 L beakers
- Analytical balance with an accuracy of ± 0.1 mg
- Disposable pipettes
- Hot plate
- Watch glasses (small and large)
- 50 mL centrifuge tubes
- Centrifuge (4000-4500 rpm)
- Hot plate with magnetic stirrer

- Magnetic stirrers (small and large)
- Tweezers
- 35 mm petri dishes
- Ultra-sonic bath
- Syringe filters (0.45 µm 25 mm dia.)
- 5 mL syringes
- 80 mL vials
- 0.1 µm Millipore "VV" membrane filter (25 dia. mm)
- Vacuum filtering system (Gelman filtering apparatus or Büchner flask, filter paper holder, vacuum pump)
- Meker bunsen burner

## 7.4. Reagents

- $^{133}$Ba tracer solution containing 1 kBq/g $^{133}$Ba.
- $^{133}$Ba filter source standard spiked with 100 Bq $^{133}$Ba.
- Nitric acid ($HNO_3$ 70%)
- Hydrochloric acid (HCl 32%)
- Hydrogen peroxide ($H_2O_2$ 30%)
- Perchloric acid ($HClO_4$ 60-70%)
- Ammonia ($NH_4OH$ 25%)
- Water (deionised water; resistivity = 18.2 MΩ.cm)
- 95 or 99% ethanol
- Sulfuric acid ($H_2SO_4$ 95-99%)
- Sodium sulfate ($Na_2SO_4$)
- Sodium hydrogen sulfate ($NaHSO_4$)
- Lead(II) nitrate ($Pb(NO_3)_2$)
- Sodium hydroxide (NaOH)
- Acetic acid ($CH_3COOH$)
- Diethylenetriamine-pentaacetic acid pentasodium ($Na_5DTPA$)
- Thymol blue indicator
- 70% $NaHSO_4$
  Dissolve 70 g of $NaHSO_4$ 100 mL of water
- 50% ethanol
  Mix 1 part water and 1 part 95 or 99% ethanol
- 20% $Na_2SO_4$
  Heat 600 mL of water in a beaker on a stirrer hot plate; whilst stirring add 200 g of $Na_2SO_4$ in small amounts until dissolved; make solution up to 1L with water.
- 4% $Na_2SO_4$
  Dilute 100 mL of 20% $Na_2SO_4$ to 500 mL with water
- 10 mg/mL Pb carrier
  Dissolve 16 g of $Pb(NO_3)_2$ in 1 L of 0.1M HNO3
- 10M NaOH
  Dissolve 200 g of NaOH in 500 mL of water (in a plastic beaker)
- 0.2 M $Na_5DTPA$
  Dissolve 30g of NaOH in 300 mL of water in a plastic beaker by stirring on a mechanical stirrer. Continue stirring and add 39.3 g $Na_5DTPA$ (Merck Triplex V) until dissolved, then dilute to 500 mL with water.
- 1:1 acetic acid
  Mix 1 part water and 1 part acetic acid
- $BaSO_4$ seeding solution (containing 0.125 mg/mL Ba)
  Weigh out 0.0113 g $BaCl_2.2H_2O$ to a 250 Erlenmeyer conical flask. Add 1 mL of water to dissolve the salt. Add 10 mL 70% $NaHSO_4$ plus one drop conc. $HClO_4$. Evaporate carefully over a Meker bunsen burner while stirring until the BaSO4 has dissolved. Increase the heat and continue swirling over the burner until most of the excess $H_2SO_4$ has been removed and a pyrosulphate fusion is obtained. Cool to room temperature

while rolling the melt around the side of the flask. Add 50 mL 20% $Na_2SO_4$. Swirl the flask until the cake is completely dissolved. Transfer to a glass bottle. Shake vigorously and sit in an ultrasonic bath just prior to use.

# 8. Instructions

A flow chart for this process is included in Appendix A.

2. Weigh 1-3 g solid sample or 800g aqueous sample, into beakers labelled with unique logging IDs (see Reference)
3. Add $^{133}Ba$ tracer and $Ba^{2+}$ carrier (if necessary). $^{133}Ba$ tracer is added to determine the activity of $^{226}Ra$ in the samples and the chemical recoveries.

For liquid samples, which have very low concentrations of soluble ions (e.g. rainwater, ice samples etc.), add 1mL of a 500 ug/mL $Ba^{2+}$ carrier solution. For liquid samples with higher ion concentrations (e.g. groundwater samples) use a smaller amount of carrier, e.g. 0.2 mL (=100 ug of $Ba^{2+}$). Note: $Ba^{2+}$ carrier is not normally added to soil samples (if in doubt ask the supervisor).

4. Digest the solid sample (see Reference).
5. If the sample is phosphogypsum, gypsum or similar material, then fusion is the appropriate Total Dissolution (see Reference).
6. Concentrate the radionuclides in the dissolved solid samples or water samples by Manganese Dioxide co-precipitation (see Reference).
7. Dissolve the precipitate in a minimum volume of conc. $HNO_3$ and $H_2O_2$. Dilute to ~ 800 mL with reagent water in a 1L glass beaker.


IMPORTANT – If continuing from a $^{210}Po$ auto-deposition and the original sediment sample contained a large quantity of marine shells (i.e. high calcium component), reduce the Ca loading by evaporating the sample with 10 mL conc. $HNO_3$ then perform a Manganese Dioxide co-precipitation before proceeding any further.

8. Otherwise, transfer the solution from the $^{210}Po$ auto-deposition step into a 1L beaker and dilute to 800 mL with reagent water. Place a magnetic stirrer in the beaker.
9. While stirring rapidly on a magnetic stirrer, slowly add 20 mL conc. $H_2SO_4$. Caution: $H_2SO_4$ is highly corrosive, handle with extreme care. Refer to Safety Data Sheet (SDS) for more details on safe handling procedure.
10. Then add 100 mL 20% $Na_2SO_4$.
11. Slowly add with stirring 10 mL 10 mg/mL $Pb^{2+}$ carrier in 0.1 M $HNO_3$ from the burette placed above the beaker.
12. Allow the Pb/Ba/Ra sulphate precipitate to settle overnight.

If a large quantity of white crystals form (i.e. $CaSO_4$) you may have to abandon the analysis, consult the lab supervisor. Refer to point 4 in the Precautions section of this document.

13. Carefully and slowly decant the supernatant. Ensure minimal loss of the Pb/Ba/Ra sulphate precipitate.

14. Transfer the white precipitate to a 50 mL centrifuge tube with 50% ethanol, if necessary use a clean plastic scraper to aid the transfer of the precipitate from the sides of the beaker.
15. Centrifuge at 4000-4500 rpm for 5 minutes to pack down the precipitate.
16. Decant the supernatant to waste, being very careful not to lose any of the precipitate.
17. Again wash the walls of the beaker with 50% ethanol, collecting any remaining precipitate in the centrifuge tube.
18. Centrifuge to pack down the precipitate.
19. Discard the supernatant.
20. Add 5 mL 0.2 M $Na_5$DTPA plus 1 drop of thymol blue.
21. If necessary, add drops of 10 M NaOH to give a pH >9 (deep blue colour), shake to dissolve any precipitate stuck to the walls of the centrifuge tube.
22. Warm then suspend the tube in an ultrasonic bath for 30 minutes to dissolve all the sulphate precipitate.
23. Add 2 drops of methyl red indicator.
24. Pass through a 0.45 µm disposable membrane filter into a cleaned 70 mL polycarbonate vial.
25. Add 5 mL 4% $Na_2SO_4$ to the centrifuge tube. Cap the tube and shake briefly to collect residual $Na_5$DTPA.
26. Pass through the 0.45 µm filter into the vial. The solution is green at this step.

The method may be stopped at this step. However, if the analyst continues, the remaining steps must be completed on the same day.

27. Ensure the $BaSO_4$ seeding suspension has been ultra-sonicated for at least 15 minutes.
28. Simultaneously, add 2 mL of 1:1 acetic acid/water and 1 mL $BaSO_4$ seeding suspension, which has been ultra-sonicated. Cap the vial and mix well. The solution should be pink at this step.
29. Sit the vial in cold water or in a fridge for at least 30 minutes.
30. Mount a smooth-surfaced Millipore “VV” membrane filter in a lock-seal Gelman filter apparatus attached to a vacuum pump (make sure the shiny gridded surface is face up).
31. Rinse the filter with a little 50% ethanol, allow to drain before proceeding.
32. Swirl the vial containing the colloidal Ba/Ra sulphate precipitate and pour into the filter funnel, allow the supernatant to drain away completely before proceeding.
33. Rinse the vial and filter funnel walls with a little 50% ethanol to ensure collection of all the precipitate on the filter.

If visible crystals are present on the filter paper try dissolving them with a little water added dropwise directly on top of the crystal whilst maintaining suction. If this doesn’t work try a little ethanol instead. As a last resort large crystals or other debris can be physically removed by blowing across the surface of the dried filter paper.

34. Dissassemble the filter unit.
35. Set the filter face up in a small polystyrene petri dish (labelled with Sample ID, “Ra” and the date the source was prepared). Mark the top perimeter of the filter with a black dot (not on the precipitate).

36. Place the petri dish containing the filter on top of a HPGe gamma detector and collect a gamma spectrum for 10 minutes, measuring the recovery of $^{133}$Ba via the 356 keV peak. Also count the $^{133}$Ba filter source standard to calibrate the detector efficiency.
37. Using tweezers, carefully stick each Ra/Ba source filter onto a carbon tab, already labelled with the sample number on one side.
38. Take the filter sources to the Alpha Spectrometry laboratory.
39. Analyse $^{226}$Ra by alpha spectrometry (see Reference).
40. If the Ra alpha spectrum from a sample shows poor resolutions (broad peaks, peaks overlapping), it may be due to interfering materials co-precipitating with the Ba and Ra. The filter source can be purified by following the steps outlined below.
41. Place the Ra/Ba filter source in a 70 mL polycarbonate vial.
42. Add 5 mL 0.2 M $Na_5$DTPA, 1 drop of thymol blue and a few drops of 10M NaOH until the solution turns blue.
43. Place the vial in an ultrasonic bath for 15-30 minutes to dissolve all the sulphate precipitate.
44. Take the filter and the carbon tab out with a pair of tweezers, rinse them with a small amount of water over the vial. The filter and carbon tab can be discarded.
45. Repeat steps 22 to 38. Record this purification step in the Radium Analysis Data Sheet.

# 9. Records

46. Sample identification and all weights/data shall be recorded on a Radium Analysis Data Sheet (see Appendix B).
47. On completion of the whole analysis the Radium Analysis Data Sheet is transferred to the project file containing all the sample information.

The following records are to be maintained for Radium Chemical Isolation.

| File Number | Title | Type | Storage Location | Retention |
|---|---|---|---|---|
| | | | | |

# 10. References


- Environmental Radioactivity Measurement Centre (ERMC) Safety Assurance Committee (SAC) form.
- Sill, C.W., Puphal, K.W., Hindman, F.D., Simultaneous determination of alpha emitting nuclides of radium through californium in soil, Anal. Chem. 46 12 (1974) 1725-1737.
- IAEA/AQ/19-IAEA Analytical Quality in Nuclear Applications Series No. 19. Analytical Methodology for the Determination of Radium Isotopes in Environmental Samples (2010).
- Total Dissolution using HF (ANSTO Quality document I 3332)
- Polonium chemical isolation (ANSTO Quality document I 3329)
- Manganese dioxide co-precipitation (ANSTO Quality document I 2806)
- Operation of Ortec Alpha Spectrometers (ANSTO Quality document I 3321)
- Sample Logging (ANSTO Quality document I 2805)

# Appendix A: Radium Analysis Flow Chart

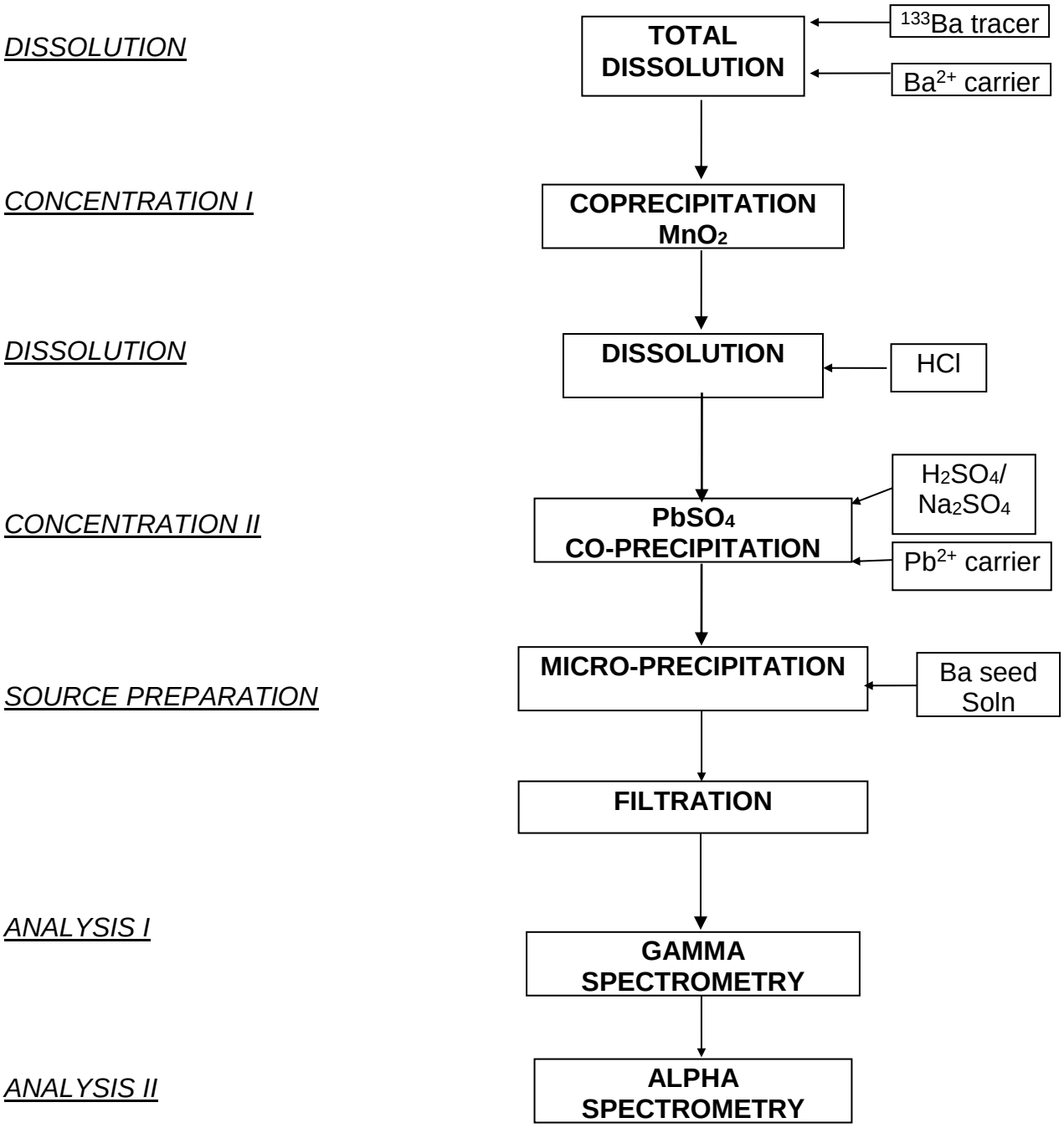

**APPENDIX C: ERMC POLONIUM CHEMICAL ISOLATION**

# Purpose

This instruction establishes the Isotope Tracing in Natural Sytems (ITNS) requirements for the analysis of polonium-210 ($^{210}$Po), undertaken at ANSTO Environmental Radioactivity Measurement Centre (ERMC).

The instruction explains how polonium isolated by the auto-deposition method onto a silver disk and analysed by alpha spectrometry (see Appendix A).

# Scope

This analytical scheme has been designed for the determination of $^{210}$Po in waters, rocks, soils, sediments and biological material.

## Document History

This instruction replaces the VI-3329 quality document. This is a revision to add extra information on how to prepare all the reagents used in this analytical procedure and more relevant References.

### Table of Contents



# 11. Pre-Requisites

## 11.1. Precautions

48. If multiple elements are being analysed, read all associated instructions to avoid chemical/process incompatibilities.
49. If following on from the Lead-210 dating sample preparation method (see Reference) then processing commences at step 3 (in section 2. Instruction).
50. The polyethylene holder for the silver disk must be decontaminated in EDTA solution, then thoroughly washed in reagent water to remove all EDTA residues.

51. It is essential to record the date of the separation of $^{210}$Po from its $^{210}$Bi/$^{210}$Pb parents. The elapsed time (in units of 0.5 days) from separation to the mid-date of the counting period is used to compute $^{210}$Po specific activities in the sample. If $^{208}$Po tracer has been used (usually reserved for $^{210}$Pb estimation by $^{210}$Po ingrowth) the specific activity should be recalculated periodically to make the entry of time elapsed since re-calibration conveniently short.

## 11.2. Responsibility

52. The analyst shall be responsible for:
    a. performing all operations in a safe manner, see the ERMC Safety Assurance Committee (SAC) form (see Reference),
    b. applying the best quantitative practices in handling/transferring solutions,
    c. ensuring all apparatus is cleared away and stored on completion of analysis,
    d. recording any difficulties with or changes to this instruction on the corresponding Polonium Analysis Data Sheet (see Appendix B).

## 11.3. Sample collection, preservation and handling

53. All containers used in this procedure must be pre-washed with detergent, acid and reagent water.
54. Soil samples are collected in cleaned plastic or glass containers, using clean utensils.
55. Aqueous samples are collected in cleaned plastic bottles, and acidified to below pH 2 with A.R grade nitric acid.

## 11.4. Apparatus and materials

- 150 mL glass beakers
- Analytical balance with an accuracy of ± 0.1 mg
- Disposable pipettes
- Hot plate with magnetic stirrer
- Magnetic stirrers (small and large)
- Silver disks and holders
- Narrow range pH strips 0-6
- Tweezers
- 30 mm petri dishes

## 11.5. Reagents

- Certified polonium-209 ($^{209}$Po) tracer solution containing 2 Bq/g $^{209}$Po
- Hydrochloric acid (HCl 32%)
- Ammonia ($NH_4OH$ 25%)
- Ascorbic acid ($C_6H_8O_6$)
- Hydroxylammonium chloride ($NH_2OH$. HCl)
- Bismuth(III) nitrate pentahydrate (Bi(NO3)3.5H2O)
- Citric acid ($C_6H_8O_7$)
- Cresol red indicator
- 0.1M HCl
  Add 10 mL of 32% HCl to about 600 mL of MQ water in a 1 L measuring cylinder and make up to 1L.
- 1.0M citric acid
  Dissolve 210 g of citric acid in water and make up to 1 L.
- 10 mg/mL Bi carrier
  Dissolve 5.8 g of $Bi(NO_3)_3.5H_2O$ in 250 mL of 2M $HNO_3$.
- 95 or 99% Ethanol ($C_2H_6O$)
- Water (deionised water; resistivity = 18.2 MΩ.cm)

# 12. Instructions

This process is outline in the flow chart in Appendix A.

56. $^{209}$Po tracer must be added to the sample at the beginning of the sample preparation. The amount of $^{209}$Po tracer to add is usually 0.2 Bq (0.1g of 2 Bq/g $^{209}$Po solution). Record sample quantity used and tracer amount in the Polonium Analysis Data Sheet (see Appendix B). Solid materials, such as sediment, soil and biological samples, must be digested before proceeding with this method (see Reference). In the case of water samples, Manganese Dioxide Co-precipitation (see Reference) must be undertaken to concentrate the polonium in the samples.
57. Convert the evaporated polonium fraction to $Cl^-$ form by evaporating several small volumes of conc. HCl.
58. Prepare silver disks and assemble polyethylene disk holders (usually done the day before).

START HERE if following on from Lead-210 dating sample preparation (see Reference).

59. Add 30 mL of 0.1M HCl and 50mL reagent water (or 80 mL of 0.04M $HNO_3$). Place a stirring bar in each beaker, labelled with a unique logging ID, and place on a hot plate-stirrer unit. Turn the stirrer on and heat to temperature between 70-90°C.The residues should dissolve up.
60. Add about 0.2 g of ascorbic acid (approximately 0.5 $cm^3$ volume) to each sample and wait for at least 3 minutes before proceeding with the next step. This will reduce Fe(III) to Fe(II), which will not deposit on the surface of the silver disks. In some cases the solution goes black following the addition of ascorbic acid which indicates not all of the Fe(III) has been reduced to Fe(II). If this occurs, add extra ascorbic acid, in small amounts, until the solution is colourless.
61. Add 100 µL 1.0M citric acid solution to complex trace iron and chromium, which are oxidising agents.

This method is subject to interference from oxidising agents such as Fe(III) and Cr(VI) as well as some chelating agents and other elements which co-deposit onto silver.

62. Add 10 mg $Bi3^{+}$ holdback carrier to inhibit the autodeposition (i.e. co-deposition) of Bismuth.

There are four bismuth alpha emitters however due to their short half-life all decay to insignificance within 24 hours. Therefore the silver disks should not be counted within 24 hours of preparation. As $^{210}Bi$ decays principally by beta emission (>99%) the alpha spectrum would not be observed. If aged $^{228}Th$ was used as a yield tracer then $^{212}Bi$ (half-life = 60.5 minutes) would be present (daughter of $^{232}Th$) however once deposited it is unsupported and thus not present after 24 hours.

63. Weigh out about 1 g of hydroxylammonium chloride for each sample in a small container.
64. Adjust the pH to 1.5 with conc. $NH_4OH$ using cresol red indicator and/or narrow range pH paper.

Sometimes an opaque precipitate may form. This is likely to be bismuth oxychloride, which is formed by the decomposition of bismuth chloride; it has an insignificant effect on the deposition of polonium. Hence: $Bi^{3+} + 3Cl^{-} \Rightarrow BiCl_3$

$BiCl_3 + NH_4OH \Rightarrow BiOCl\ (s) + NH_3 + 2HCl$

65. Add rapidly the 1g hydroxylammonium chloride and immediately float the polyethylene holder containing the silver disk. Place the disk holder at an angle to prevent bubbles forming on the silver disk surface.

Hydroxylamine hydrochloride ($NH_2OH.HCl$) is used as the reductant.

66. Place an inverted watch glass (used in the digestion step) on top of the beaker to reduce solution losses due to evaporation.
67. Autodeposit polonium onto the silver disk for approximately 4-6 hours (i.e. assuming that this procedure, starting from step 4, was started first thing in the morning the autodeposition can be left on for most of the day. The figure of 4-6 hours is somewhat arbitrary and continuously mixed solutions can be plated in under an hour however generally longer is better).

Pay special attention to steps 13 and 14

68. Remove bubbles trapped underneath the disk holder by periodically spinning the disk holder. Failure to do this results in less than optimal autodeposition due to the plating solution being unable to make good contact with the disk surface. Check the stirrer bars are not spinning to fast. The silver disk holders should float steadily without too much rocking.
69. Maintain the volume in the beaker by periodic addition of reagent water. If the volume is allowed to decrease the remaining solution will become too acidic, resulting in less than optimum conditions.

70. When the autodeposition is completed, remove the silver disk holder.
71. Rinse the silver disk holder well with reagent water and collect washings in the deposition beaker.
72. Disassemble the disk holder.
73. Rinse the silver disk with reagent water and again collect washings.
74. Hold the silver disk over a clean waste container and rinse with 95% ethanol (do not collect washings). If you drop the disk into the waste container carefully pick-up the disk by the edges taking care not to scratch the surface and rinse very thoroughly with water and ethanol (do not collect either the water or ethanol washings).
75. Drain the silver disk on a disposable tissue, without touching the deposited surface. Allow the disk to air dry.
76. Label the silver disk on the backside with sample ID.
77. Transfer to a small petri dish (labelled with sample ID, “Po” and date of autodeposition) for transport and storage.
78. Determine the activity of $^{210}$Po by counting the prepared silver disk sources by alpha spectrometry (see Reference).
79. If the Po alpha spectrum from a sample shows poor resolutions (broad peaks, peaks overlapping), it may be due to interfering materials plating onto the silver disk. Place the silver disk in a 100 mL beaker.
80. Add 10 mL of 6M HCl into the beaker.
81. Place the beaker in an ultrasonic bath and ultrasonicate for 15 minutes. This step should leach out (remove) interfering materials plated onto the silver disk, but not the polonium itself. Do not leave the silver disk longer than 15 minutes in the acid solution, otherwise the silver could dissolve up.
82. Take the disk out of the beaker, follow steps 20 to 23. Record this purification step in the Analysis Data Sheet (Appendix B).

# 13. Records

83. Sample identification and all masses/data shall be recorded on a Polonium Analysis Data Sheet (Appendix B).
84. On completion of the whole analysis the Polonium Analysis Data Sheet is transferred to the project file containing all the sample information.

The following records are to be maintained for Polonium Chemical Isolation.

| File Number | Title | Type | Storage Location | Retention |
|---|---|---|---|---|
| | | | | |

# 14. References


- Environmental Radioactivity Measurement Centre (ERMC) Safety Assurance Committee (SAC) form.
- Matthews, K.M., Kim, C.K., Martin, P, 2007. Determination of $^{210}$Po in environmental materials: A review of analytical methodology. Applied Radiation and Isotopes 65, 267–279.
- Total Dissolution using HF (ANSTO Quality document I 3332)
- Lead-210 dating sample preparation (ANSTO Quality document I 3331)
- Manganese dioxide co-precipitation (ANSTO Quality document I 2806)
- Operation of Ortec Alpha Spectrometers (ANSTO Quality document I 3321)

- Sample Logging (ANSTO Quality document I 2805)

# Appendix B: Polonium Analysis Flow Chart

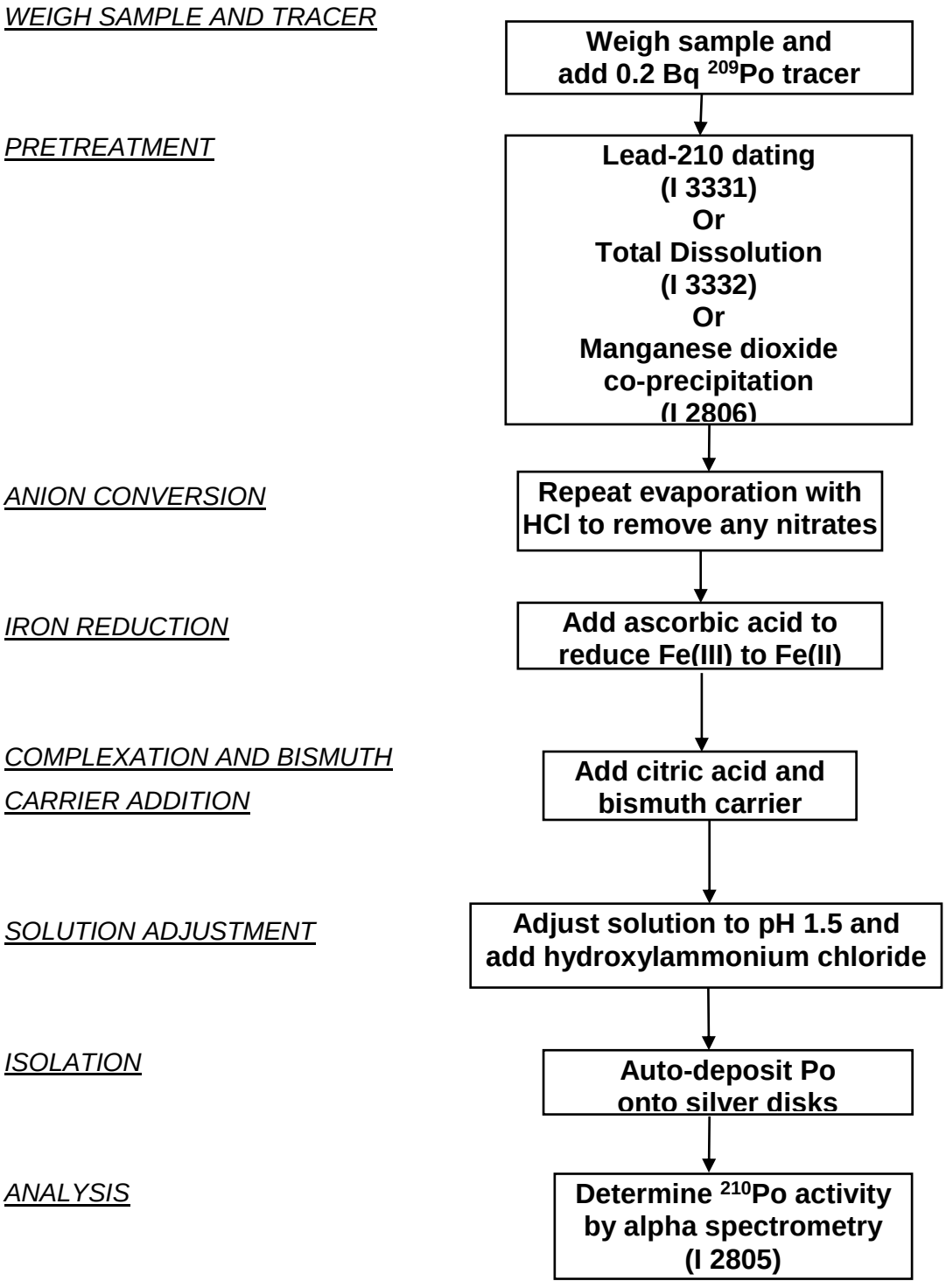

**APPENDIX D: LEAD-210 DATING SAMPLE PREPARATION**

# Purpose

This instruction establishes the Isotope Tracing in Natural Sytems (ITNS) requirements for the determination of sedimentation rate by the lead-210 ($^{210}$Pb) method, undertaken at ANSTO Environmental Radioactivity Measurement Centre (ERMC).

The instruction explains how sediments are processed prior to their analysis for polonium-210 ($^{210}$Po) and radium-226 ($^{226}$Ra) by alpha spectrometry. $^{210}$Po and $^{226}$Ra activities in sediment cores are analysed for the determination of sedimentation rates. See Appendix B showing the lead-210 pathway in the environment.

# Scope

This sample treatment scheme has been designed specifically for determining the sedimentation rate(s) of sediment. The method is not appropriate for the analysis of water samples.

## Document History

This instruction replaces the VI 3331. This version contains minor revision.

### Table of Contents



# 15. Pre-Requisites

## 15.1. Precautions

85. Samples must be handled in a working fume cupboard during acid digestion.
86. Low level radioactive tracers are used in this procedure. See the ERMC Safety Assurance Committee (SAC) form on safe handling of radioactive tracers (see Reference).

## 15.2. Responsibility

87. The analyst shall be responsible for:
    a. performing all operations in a safe manner (refer to the ERMC SAC form),
    b. applying the best quantitative practices in handling/transferring solutions,
    c. ensuring all apparatus is cleared away and stored on completion of analysis,
    d. recording any difficulties with or changes to this instruction on the corresponding $^{210}$Po and $^{226}$Ra analysis data sheet (Appendix C).

## 15.3. Apparatus and Materials

88. Drying oven,
89. Analytical balance with an accuracy of ± 0.1 mg,
90. Hot plate,
91. IR thermometer,
92. Mortar and pestle (or ring grinder),
93. Beakers of assorted sizes,
94. Watch glasses,
95. Pipettes,
96. Measuring cylinders,
97. Centrifuge, centrifuge tubes.

## 15.4. Reagents

All reagents are analytical reagent grade or better unless otherwise stated.

98. Nitric acid ($HNO_3$ 70%),
99. Hydrochloric acid (HCl 32%),
100. Hydrogen peroxide ($H_2O_2$ 30%),
101. 2M $HNO_3$ – add 127 mL of 32% HNO3 into a 1L measuring cylinder containing 300 mL of water, make up to 1L with water,
102. 6M HCl – add 589 mL of 32% HCl into a 1L measuring cylinder containing 300 mL of water make up to 1L with water,
103. Water (deionised water; resistivity = 18.2 MΩ.cm).

# 16. Instructions

A flow chart for this process is included in Appendix A.

104. If the samples arrive in the laboratory unprocessed, straight from a core, determine the dry bulk density of each sample and dry at 60°C before proceeding (contact one of the laboratory staff). If the samples have been dried and crushed proceed to the next step.
105. Weigh 0.2 - 2 g of sediment accurately, into a 150 mL beaker, labelled with a unique logging ID. Record the weights in the Polonium & Radium data sheet (Appendix C).
106. Add approximately 5000 dpm of $^{133}$Ba and 10 dpm of $^{209}$Po mixed tracer solution. Typically the mixed $^{133}$Ba and $^{209}$Po tracer stock will have a concentration close to 50 dpm/ml of $^{209}$Po and 25,000 dpm/g $^{133}$Ba, so that the addition of 0.2 g of stock solution (equivalent to about 14-15 drops) weighed by difference and accurate to 5 decimal places will be sufficient to provide the 10 dpm of $^{209}$Po tracer and 5000 dpm of $^{133}$Ba tracer. When taking out a tracer bottle from the cupboard always place the bottle on a tray lined with disposable wipes (to contain any accidental spills).

It is essential that the lid on the tracer bottle be replaced immediately after use to prevent any evaporation of the stock solution as this would result in a stock solution of unknown concentration. Always use a new pipette at each session when tracers are dispensed as used pipettes will contain residual activity of a higher concentration (due to evaporation of solvent) than the stock solution in the bottle.

107. Ensure the fume cupboard is working properly. Place a hot plate in the fume cupboard, cover the surface with a sheet aluminium foil and turn it on to heat up.


From now on, all the steps must be undertaken in the fume cupboard.

108. Slowly add (from a wash bottle) between 10-20 mL of 2M $HNO_3$ into each beaker. The whole sample should be dispersed in the 2M $HNO_3$. A vigorous reaction may occur if the samples contain high concentration of carbonates (usually from shells). Rinse any sample sticking to the wall of the beaker with 2M $HNO_3$ from a wash bottle.

109. Place each beaker on the hot plate. Leave them on the hot plate for at least 5 minutes at 40-50°C. If the samples do not react vigorously go to step 7, otherwise go to step 8. Use an IR thermometer to check the sample temperature.

110. If any of the samples react vigorously (foams over spilling from the beaker, usually from high concentration of organics), take the sample off the hot plate immediately, add a drop of n-octanol (surfactant for reducing foaming) and let it cool down, dilute with 10-20 mL of water and place it back on the hot plate. Leave them on the hot plate until minimal reaction is observed.

111. Take the samples off the hot plate to cool down, and then slowly add 10 mL of conc. $HNO_3$. Swirl the sample around and slowly add another 15 mL. Vigorous reactions may occur when adding conc. $HNO_3$ at this stage, therefore ensure the samples have cooled down and always add the concentrated acid in small aliquots.

112. Rinse any sample sticking to the wall of the beaker with 2M $HNO_3$ from a wash bottle.

113. Place the samples back on the hot plate. Watch if any of the samples react too vigorously. Add a few drops of n-octanol if this occurs.

114. Check the temperature of the samples using an IR thermometer. Adjust the hotplate control so that the sample temperature is around 60°C.

115. Leave the samples on the hot plate to evaporate close to dryness. This may take a few hours. Keep checking samples during the digestion, rinse any sample sticking to the wall of the beaker with a small amount of 2M $HNO_3$, check that the sample temperature remains around 60°C.

116. Once evaporated close to dryness, let the samples cool down.

117. Add 5-10 mL of water just enough to cover the sediment on the bottom of the beaker and a few drops of $H_2O_2$. Gently swirl, to mix and collapse any bubbles that form.

118. Place each beaker on the hot plate, heat until the effervescence subsides.

119. Take the samples off the hot plate, cool and add another a few more drops of $H_2O_2$. Gently swirl the beaker.

120. Repeat steps 14 – 15. Increase the volume of $H_2O_2$ addition once the reaction becomes less vigorous. Typically a total of 25 mL of $H_2O_2$ should be added. The colour of the sample residues should appear much lighter than originally. If they appear dark and still reacting with each addition of $H_2O_2$, more $H_2O_2$ should be added. For samples with high organic contents this step may take half a day.

121. Once the reaction has subsided, and the residues appear lighter in colour, stop the addition of $H_2O_2$, and leave the samples on the hot plate to reduce to a minimal volume.

122. Label a watch glass for each beaker with the respective sample number.

123. Take the samples off the hot plate and let them cool.

124. Add 10mL $HNO_3$ and 30mL of HCl (40mL of aqua-regia) to each beaker, place a watch glass on top of the beaker and put them back on the hot plate.

The addition of HCl results in the production of an azeotrope (or constant boiling point acid composition) which dissolves all authigenic phases (oxyhydroxides, sulphides, carbonates etc.) and leaches the surfaces of clays and primary minerals.

125. Reflux for at least 4 hours, or overnight, on a hot plate. Check the temperature of the samples. Around 60°C for a 4 hour reflux, 50°C for an overnight reflux.

126. Once the reflux step is completed, determine if the samples have been digested sufficiently. If the colour of the residues appear light (creamy grey), much lighter than originally and the supernatant is yellow (not brown), the sample is likely to be have been digested sufficiently, proceed to step 24. If the colour of the residues and the supernatant are dark brown colour, the sample may need to be digested further, it may be necessary to repeat steps 8 to22 (i.e. addition of extra $HNO_3$, $H_2O_2$ and aqua regia). Discuss with the laboratory supervisor.


IMPORTANT: Before proceeding to the next step, record the colour of residues in the Polonium & Radium data sheet. The colour should be either light grey or dark brown. The lighter the colour the more likely the samples have been digested sufficiently. This information may help to explain poor results such as low sample recoveries.

127. Following the refluxing step, usually the next day, take the samples off the hot plate and let them cool. If any of the samples dried up, add 20 mL of 6M HCl, heat (and ultrasonicate if necessary) to ensure the residues dissolve up before undertaking the next step.

128. Once cooled, transfer the samples into a 50 mL centrifuges. Use 6M HCl to rinse and transfer the samples.

129. Centrifuge at 4500 rpm for 5 minutes.

130. Decant the supernatants into the original 150 mL glass beakers.

131. Add another 15mL of 6M HCl into each centrifuge, shake it up to rinse the residues and centrifuge again at 4500 rpm for 5 minutes.

132. Decant the supernatant into the respective 150 mL glass beakers. Discard the residues in the centrifuges.

133. Place the beakers with the samples back on the hot plate to evaporate close to dryness.


IMPORTANT: When heating and evaporating ensure the samples do not exceed $60^0$C.

134. Once evaporated, rinse the wall of the beaker with 10 mL of 6M HCl and place them back on the hot plate to evaporate close to dryness.

135. Once evaporated, add about 5 mL of conc. HCl and place them back on the hot plate to evaporate close to dryness.

136. Repeat step 32 one more time to ensure the removal of any nitrates.

137. Take the samples off the hot plate and let them cool. The samples are ready for the next step.

138. Proceed as described for Polonium chemical isolation (see Reference).

139. Save the spent solution for Radium chemical isolation (see Reference).

If samples contain high concentration of calcium (e.g. Marine shell fragments) then a Manganese Dioxide Co-precipitation (see Reference) will need to be undertaken prior to proceeding with the radium isolation in order to avoid production of too thick a spectral source.

140. Add 5 mL of conc. $HNO_3$ to the spent solution and evaporate to dryness on the hot plate. This step is necessary to remove the reducing agent (hydroxyl ammonium chloride) added during the polonium autodeposition step.

141. Alternatively, Manganese Dioxide Co-precipitation can be done following step 29 (before the Polonium isolation step).

142. Determine chemical recovery of $^{226}Ra$, by counting the radium source on a gamma spectrometer to determine the $^{133}Ba$ tracer activity.

143. Determine the activities of $^{210}Po$ and $^{226}Ra$ by counting the sources by alpha spectrometry (see Reference).

144. Enter the alpha and gamma counting results into the latest Po & Ra calculations excel spreadsheet (see Reference).

145. Determine the sedimentation rate using the most current $^{210}Pb$ dating excel spreadsheet This step is done by a staff member familiar with the $^{210}Pb$ dating calculations.

# 17. Records

146. Sample identification and all weights/data shall be recorded on Polonium and Radium analysis data sheets (Appendix C) and stored in the project folder for the corresponding batch of samples. This applies to the electronic records as well as the hard copies.

147. The alpha and gamma counting results (Region of Interest (ROI) report print outs) shall also be stored in the corresponding project folder.

148. All data entries shall be checked by a second person, and signed off.

# 18. References


- Environmental Radioactivity Measurement Centre (ERMC) Safety Assurance Committee (SAC) form.
- J.D. Eakins, R.T. Morrison, A new procedure for the determination of lead-210 in lake and marine sediments., Int. J. App. Rad. Isotope. 29, 531-6, 1978.
- Ivanovich, M. & Harmon, R.S.; Uranium-Series Disequilibrium, Applications to Earth, Marine and Environmental Sciences, second edition; Clarendon Press 1992.
- Manganese dioxide co-precipitation (I 2806)
- Polonium Chemical Isolation (I 3329)
- Radium Chemical Isolation (I 3330)
- Operation of Ortec Alpha Spectrometers (I 3321)
- ERMC Sample Logging (I 2805)

# Appendix D:Sample Preparation Flow Chart

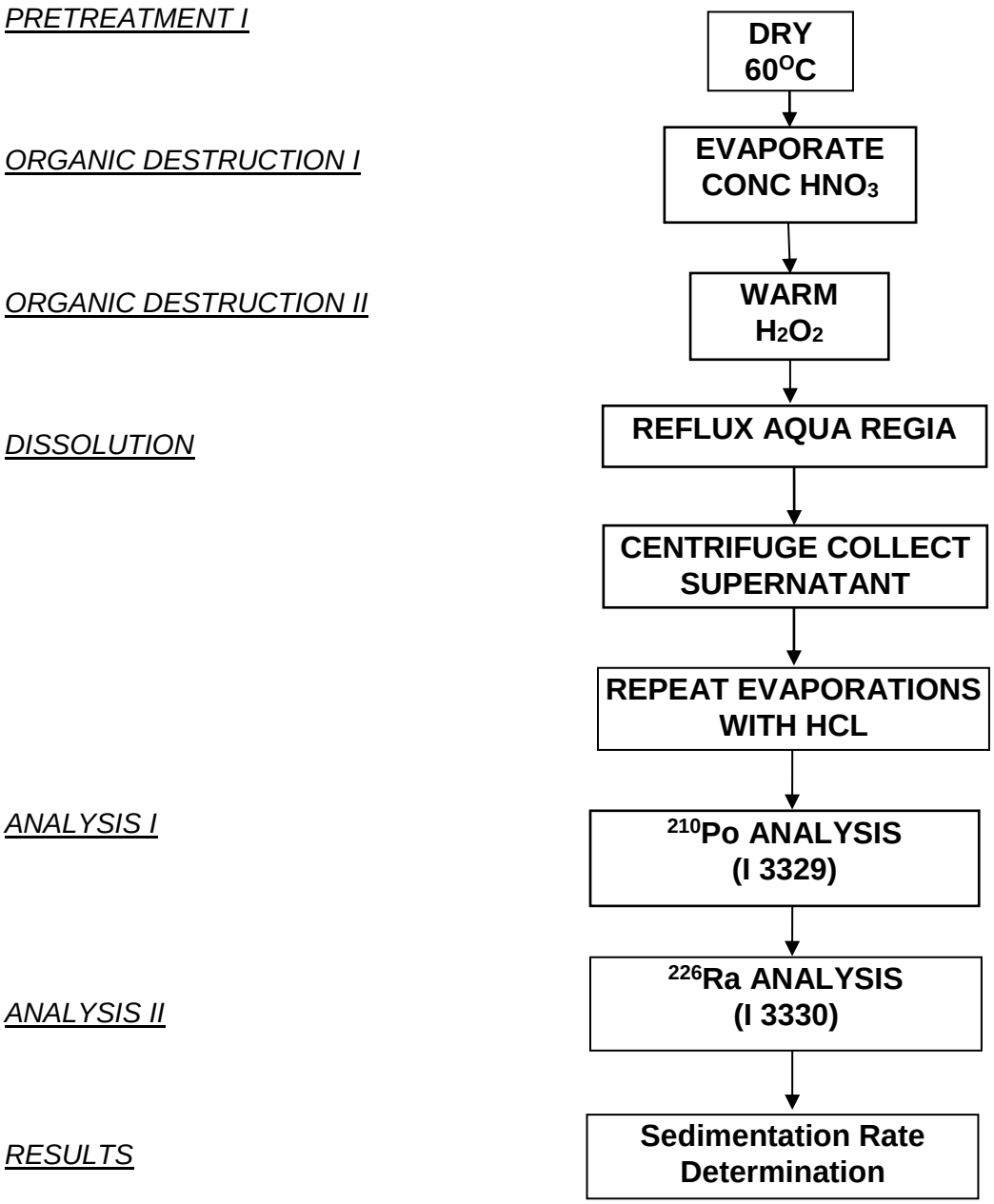

## APPENDIX E: ITRAX VALUES